LBL-4678
UC-11
TID-4500-R64

THE ENVIRONMENTAL SURVEILLANCE PROGRAM OF THE LAWRENCE BERKELEY LABORATORY

Prepared by the Staff of the Engineering and Technical Services Division

Editor: Ralph H. Thomas

April 1976

Prepared for the U. S. Energy Research and Development Administration under Contract W-7405-ENG-48

LBL-4678

THE ENVIRONMENTAL SURVEILLANCE PROGRAM OF THE LAWRENCE BERKELEY LABORATORY

Prepared by the Staff of the
Engineering and Technical Services Division
Lawrence Berkeley Laboratory

April 1976

Editor: Ralph H. Thomas

The following staff of the Engineering and Technical Services Division have contributed to the preparation of this report:

H. P. Cantelow	Safety Services Department
A. R. Smith	Health Physics Department
L. D. Stephens	Health Physics Department
R. H. Thomas	Health Physics Department
H. Wollenberg	Health Physics Department
J. Young	Safety Services Department

TABLE OF CONTENTS

ABSTRACT

The major radiological environmental impact of the Lawrence Berkeley Laboratory is due to the operation of four particle accelerators in the pursuit of fundamental research in various disciplines including biology, chemistry, medicine and physics.

Potential sources of population exposure at the Laboratory are discussed. The major source of population exposure due to accelerator operation arises from the prompt radiation field which consists principally of neutrons and photons. Release of small quantities of radionuclides is also a potential source of population exposure but is usually an order of magnitude less significant. Accelerator produced radiation levels at the Laboratory boundary are comparable with the magnitudes of the fluctuations found in the natural background radiation. Considerable effort has, therefore, been expended in understanding the magnitude of the components of natural background at the Lawrence Berkeley Laboratory, so that the magnitude of Laboratory-produced radiation may be accurately determined.

Environmental monitoring of accelerator-produced radiation and of radionuclides is carried on throughout the Laboratory, at the Laboratory perimeter, and in the regions surrounding the Laboratory. The techniques used are described.

Finally, the models used to calculate population exposure are described and discussed.

XBB 673-1730

Frontispiece I. General view of the eastern half of Berkeley with the Lawrence Berkeley Laboratory site lying at the foot of the hills.

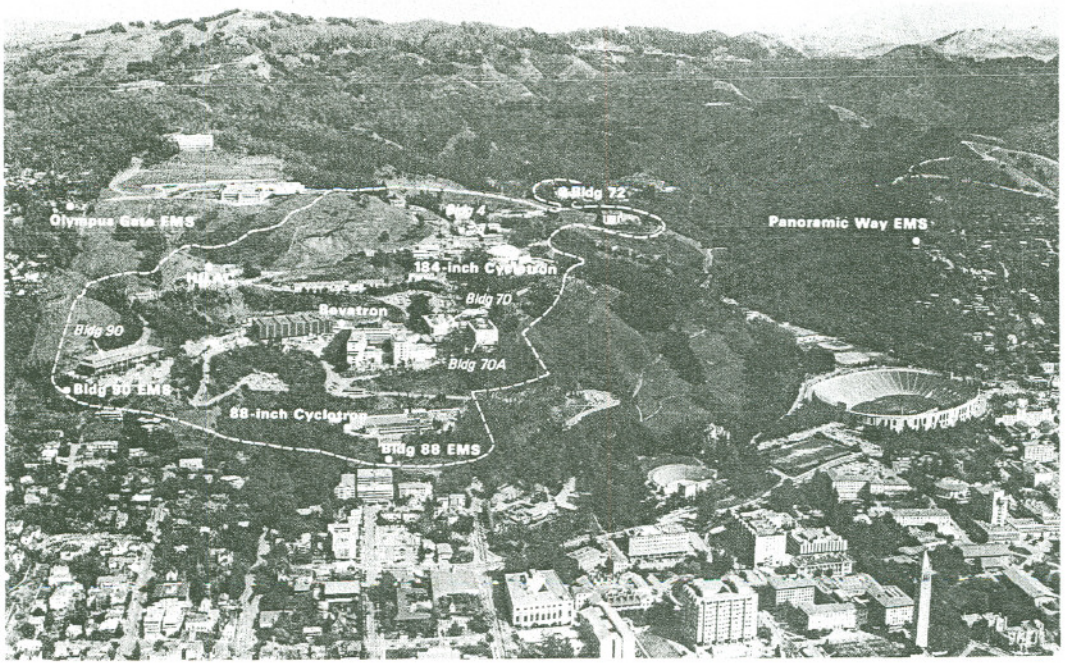

XBB 733-1830

Frontispiece II. View of the Lawrence Berkeley Laboratory and adjacent campus and city area. The perimeter of the Laboratory is outlined. The location of the four environmental monitoring stations, the accelerators, the Health Physics Building (Building 72), and the Safety Services Building (Building 4) are also shown.

1. Introduction--The Lawrence Berkeley Laboratory

1.1. General Description

The Lawrence Berkeley Laboratory, a large multi-disciplinary research institute, is located on the western slopes of the hills above the University of California and the City of Berkeley.

The Laboratory carries on a wide-ranging program of general research in the fields of physical and biological sciences. Facilities include a number of large accelerators, and various physics, chemistry, biology, and medical research laboratories.

Three particle accelerators, the Bevatron, the SuperHILAC, and the 88-Inch Cyclotron are in almost continuous operation for research purposes; one other accelerator, the 184-Inch Synchrocyclotron, is used for short periods for bio-medical studies and tumor therapy requiring alpha particles at an energy of nearly 1 GeV. The Bevatron, a large proton synchrotron, is used for physics research requiring energies of up to 6.3 GeV. The SuperHILAC is a linear accelerator capable of accelerating all natural elements up to and including uranium to energies of $\sim$8 MeV per nucleon, or a maximum energy of nearly 2 GeV per particle. This accelerator is extensively used in studies of the transuranic elements. The SuperHILAC is also used as an injector to the Bevatron, resulting in a hybrid accelerator called the Bevalac. With this instrument heavy ions may be accelerated to energies of several GeV per nucleon and applied to research in high energy physics, nuclear chemistry, radiobiology and radiotherapy. The 88-Inch sector focussed cyclotron accelerates light and medium mass nuclei to energies intermediate between that of the SuperHILAC and the Bevalac. The extremely fine energy resolution of the particle beams obtained make this accelerator

an ideal instrument for studies of nuclear structure, and its high beam intensities facilitate radioisotope production.

1.2. Location of the Laboratory

The Lawrence Berkeley Laboratory (LBL) of the University of California is situated between the 400 ft and 1000 ft levels on the western slope of the first range of hills parallel to the eastern side of San Francisco Bay. The Laboratory area is enclosed on the north and south sides by populated residential areas of the cities of Berkeley and Oakland. The major part of the Berkeley Campus of the University of California lies on the west side of the Laboratory. Higher up on the hills to the east are the Lawrence Hall of Science and the Space Sciences Laboratory; beyond them lies uninhabited land of the Tilden Regional Park. The geographical setting is shown in the frontpieces and in Fig. 1. The Laboratory is unique among high-energy accelerator laboratories in that it is contiguous with fairly densely populated areas.

1.3. Geology of the Region Around the Lawrence Berkeley Laboratory

As we shall see later (Section 1.4), the geology of the region around the Laboratory has an extremely important influence on the component of natural background due to terrestial radioactivity. Some understanding of the geology of the San Francisco Bay Area is, therefore, important in the final evaluation of the radiological impact of Laboratory operations.

Figure 2 shows a general geological map of the San Francisco Bay Area. The geology of the Laboratory site is determined by its location on the western flank of the Berkeley Hills, partly on the escarpment

XBC 7412-6205

Fig. 1. Map showing the location of the Lawrence Berkeley Laboratory and its immediate surroundings.

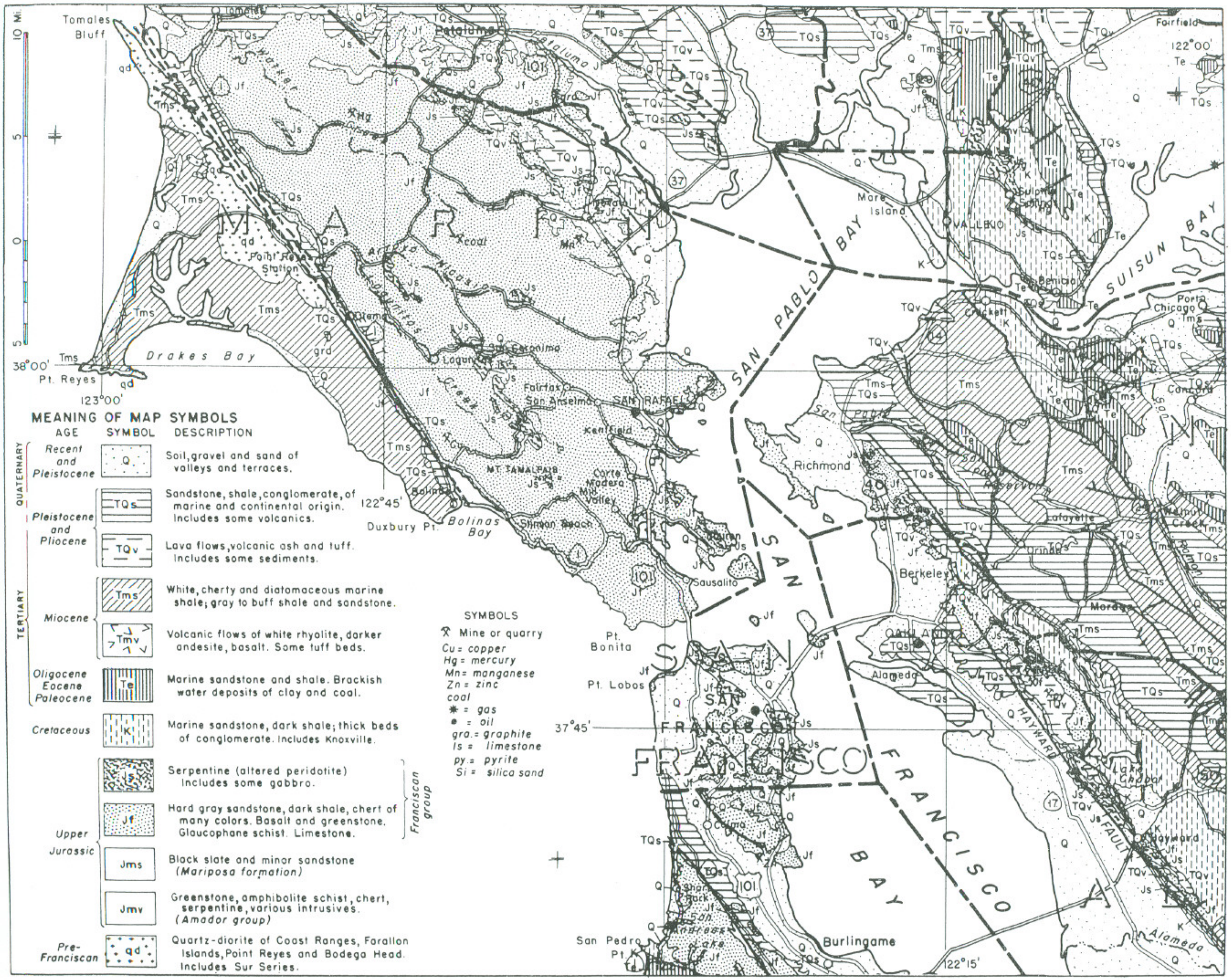

Fig. 2. Geological map of a part of the Bay Region (from Geologic Guide Book of the San Francisco Bay Counties, Bulletin 154, California Division of Mines, 1951).

afforded by the Hayward Fault zone, and partly on the northern slopes of Strawberry Canyon. The site contains numerous exposures of bedrock, as well as many zones of down-slope soil movement. Materials derived from such rock exposures have been translated downhill en masse in several places to cover differing bedrock types in portions of the site. Four major rock units underlie the area. On the west and south the site is bounded by a belt of relatively firm sandstone and conglomerates of mid- and late-Cretaceous age, known as the Chico formation. The rocks of the Chico formation are overlain by considerably younger rocks which are Miocene and Pliocene in age, and consist of well- to poorly-consolidated sandstone, siltstone, claystone and conglomerates of the Orinda Formation. The younger Orinda sediments are both interbedded and overcapped by volcanic flows of the Moraga Formation, predominately of basaltic composition at the Berkeley site. In some locations east of the Laboratory, nearer the crest of the Berkeley Hills, the volcanic rocks are more siliceous than basaltic. Thinly bedded cherts of the Claremont Formation crop out east of the main portion of the site, along the south eastern boundary of the Laboratory. These rocks are in contact with the Orinda Formation along the Wildcat Fault which transects the upper Strawberry Canyon area in a north-south orientation.

1.4. Natural Radiation Background at the Lawrence Berkeley Laboratory

1.4.1. General

The dominant environmental impact of the Laboratory's operation is radiological (See Section 2). In order to properly interpret the data obtained by the environmental radiological surveillance program,

it is important to have a good understanding of natural background at the Laboratory. Natural background at LBL amounts to between 70-110 millirem/year, made up as follows:

Natural radioactivity of surrounding earth	approx.	40-80 mr/yr[1]
Cosmic rays-μ mesons	approx.	30 mr/yr[2]
Neutrons	approx.	3 mr/yr[2]
Total	approx.	70-110 mr/yr

1.4.2. Natural Radioactivity

At the Lawrence Berkeley Laboratory, where four particle accelerators are in almost continuous operation, it is rarely possible to make measurements of the intensity of natural background with all accelerators turned off.[3] An alternative to determination of the background due to natural radioactivity *in situ* is to perform a radioassay in the laboratory on soils and rocks taken from the region of interest.[4] The γ-ray dose rates measured in nearly all terrestrial locations depend mainly on the uranium, thorium, and potassium content of the rock or soil. Thus if the content of these radioelements is determined, the γ-dose rates above the ground may be calculated.[5] Wollenberg and Smith have compared γ-ray dose rates calculated from the radioelement composition of rocks and soils with those measured in the field and obtained good agreement.[6]

To determine the range of dose rates to be expected from the soils and rocks on the Laboratory site an extensive radiogeologic survey of the natural gamma-radiation environment has been carried out.

The results of this survey are briefly described here but more complete details are given in the original reference. Some of the uncertainties in estimating γ-dose rates by this technique are also discussed.

Laboratory analysis is accomplished by using a 1600-channel pulse-height analyzer, from which 400-channel spectra covering the γ-ray energy interval 0.1 to 4.0 MeV are obtained. The spectra are analyzed by a computer program which fits standard and sample spectra over selected energy intervals channel-by-channel. An 8-inch-diameter by 4-inch-thick NaI (Tl) crystal is primarily used to measure samples packed in 6-inch diameter by 1.5-inch-thick plastic containers. Measurements of the γ-ray dose rate are also made *in situ* at sampling locations. This is done using a field-portable 3-inch by 3-inch NaI crystal detector-ratemeter system and the technique of measurement has been described in the literature. Field radiometry and subsequent laboratory gamma-ray spectrometry of soil and rock samples disclose two zones of generally differing radioactivity as is evident from inspection of the data summarized in Table 1.

Figures 3 through 5 summarize the measurements from the completed radiogeological survey.[7] Represented here are the results of the Laboratory γ-ray spectrometric analyses of 99 bedrock samples and 57 surface soil samples. This method of presentation tends to obscure some of the fine detail but does show significant general trends.

Two distinct groupings of the radioelements in both soil and bedrock samples may be seen. With one exception all the materials studied have either high concentrations of all three radioelements or low concentrations of these components. The one exception, the Claremont

Table 1. Naturally occurring radioelements and resulting exposure rates measured in samples from the LBL site.

Geologic Formation	Uranium-ppm Mean value (range)	Thorium-ppm Mean value (range)	Potassium-pct Mean value (range)	Dose-μr/hr Mean value (range)
CHICO FORMATION				
All soils (15)	2.58 ± 0.08	8.28 ± 0.32	1.76 ± 0.05	7.95 ± 0.23
	(1.98→2.93)	(5.51→10.27)	(1.25→2.26)	(5.63→9.07)
All rocks (41)	2.60 ± 0.10	8.73 ± 0.32	1.84 ± 0.04	8.26 ± 0.23
	(1.35→4.04)	(3.85→ 13.10)	(1.06→2.36)	(4.24→10.68)
CLAREMONT FORMATION				
All soils (3)	2.62 ± 0.05	3.72 ± 1.06	0.74 ± 0.20	4.61 ± 0.75
	(2.58→2.70)	(2.59→5.42)	(0.46→1.03)	(3.68→5.76)
All rocks (10)	2.99 ± 0.55	2.86 ± 0.67	0.57 ± 0.17	4.27 ± 0.82
	(1.88→7.28)	(0.44→7.77)	(0.05→1.69)	(1.69→10.38)
MORAGA FORMATION				
All soils (8)	1.30 ± 0.14	3.75 ± 0.38	0.89 ± 0.12	3.86 ± 0.38
	(0.85→1.94)	(1.49→4.59)	(0.41→1.34)	(1.91→5.03)
All rocks (21)	1.15 ± 0.07	3.14 ± 0.19	0.69 ± 0.06	3.19 ± 0.20
	(0.64→2.02)	(1.34→4.42)	(0.26→1.18)	(1.72→4.87)
ORINDA FORMATION				
All soils (21)	1.57 ± 0.11	5.08 ± 0.24	1.17 ± 0.06	5.03 ± 0.26
	(0.90→2.63)	(3.46→7.02)	(0.75→1.66)	(3.22→7.16)
All rocks (19)	1.22 ± 0.14	4.25 ± 0.52	1.06 ± 0.11	4.27 ± 0.48
	(0.44→2.31)	(1.69→9.01)	(0.43→1.84)	(1.82→8.13)

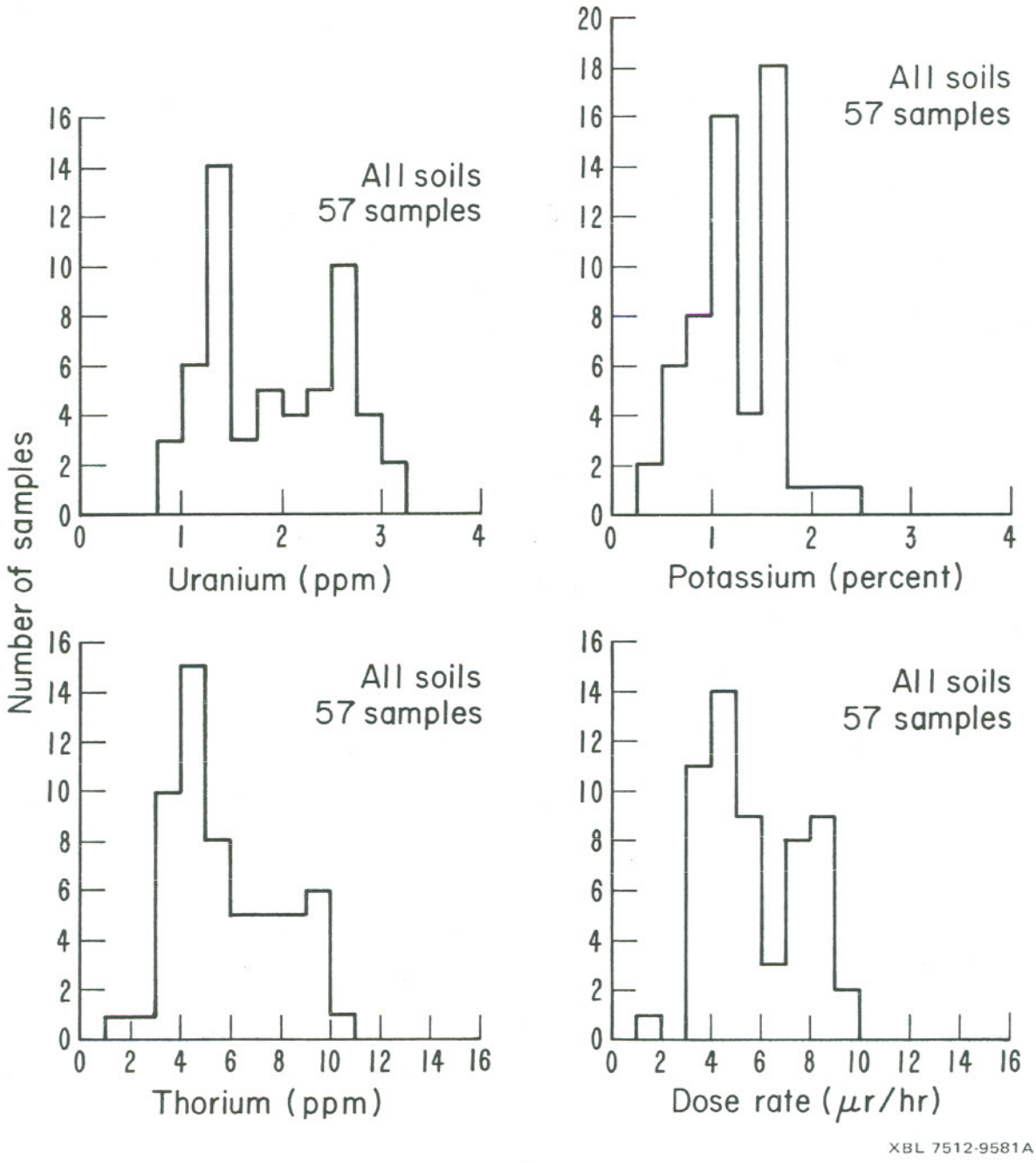

Fig. 3. Radioelement concentrations and dose rates for 57 soil samples.

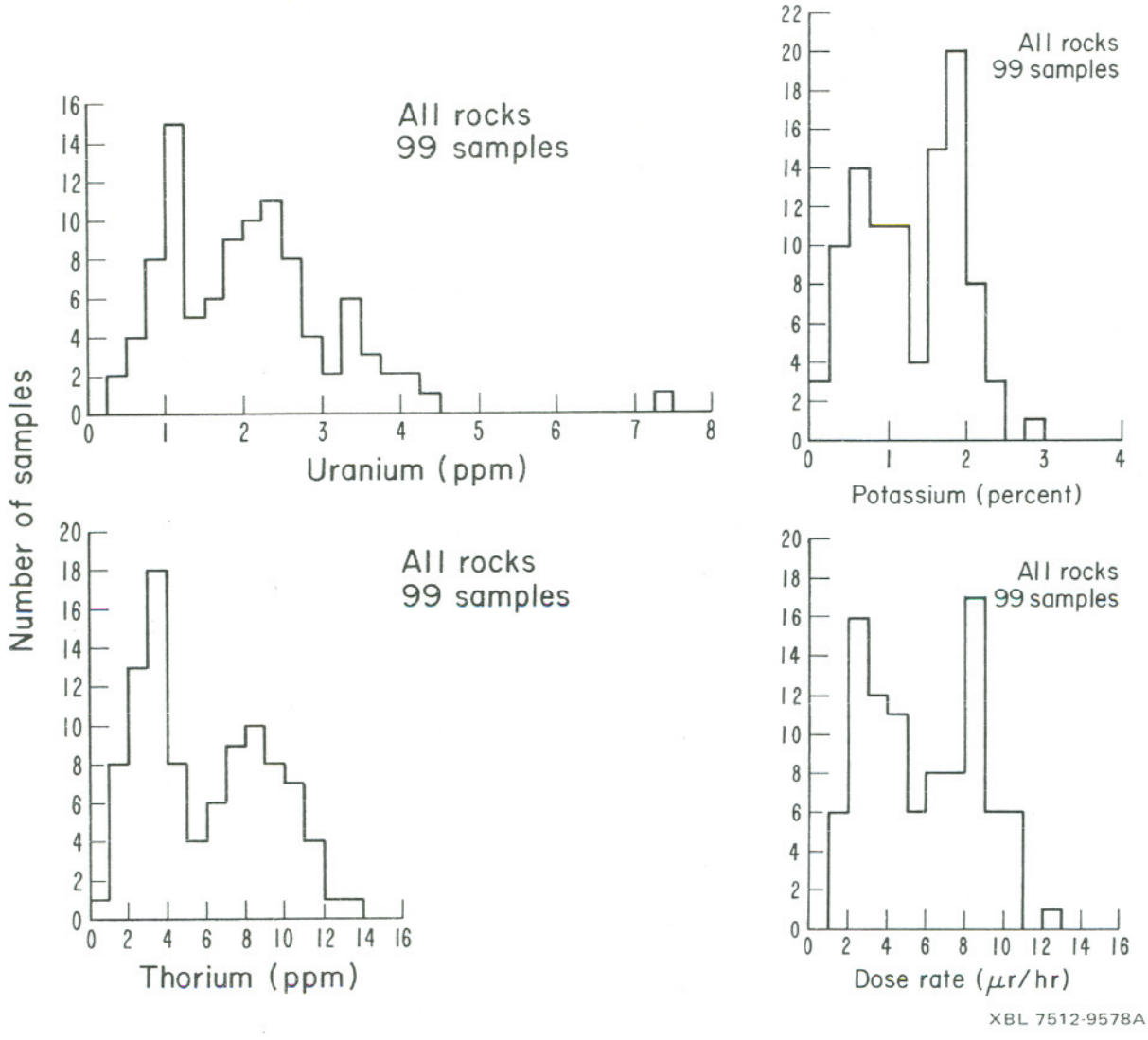

Fig. 4. Radioelement concentrations and dose rates for 99 rock samples.

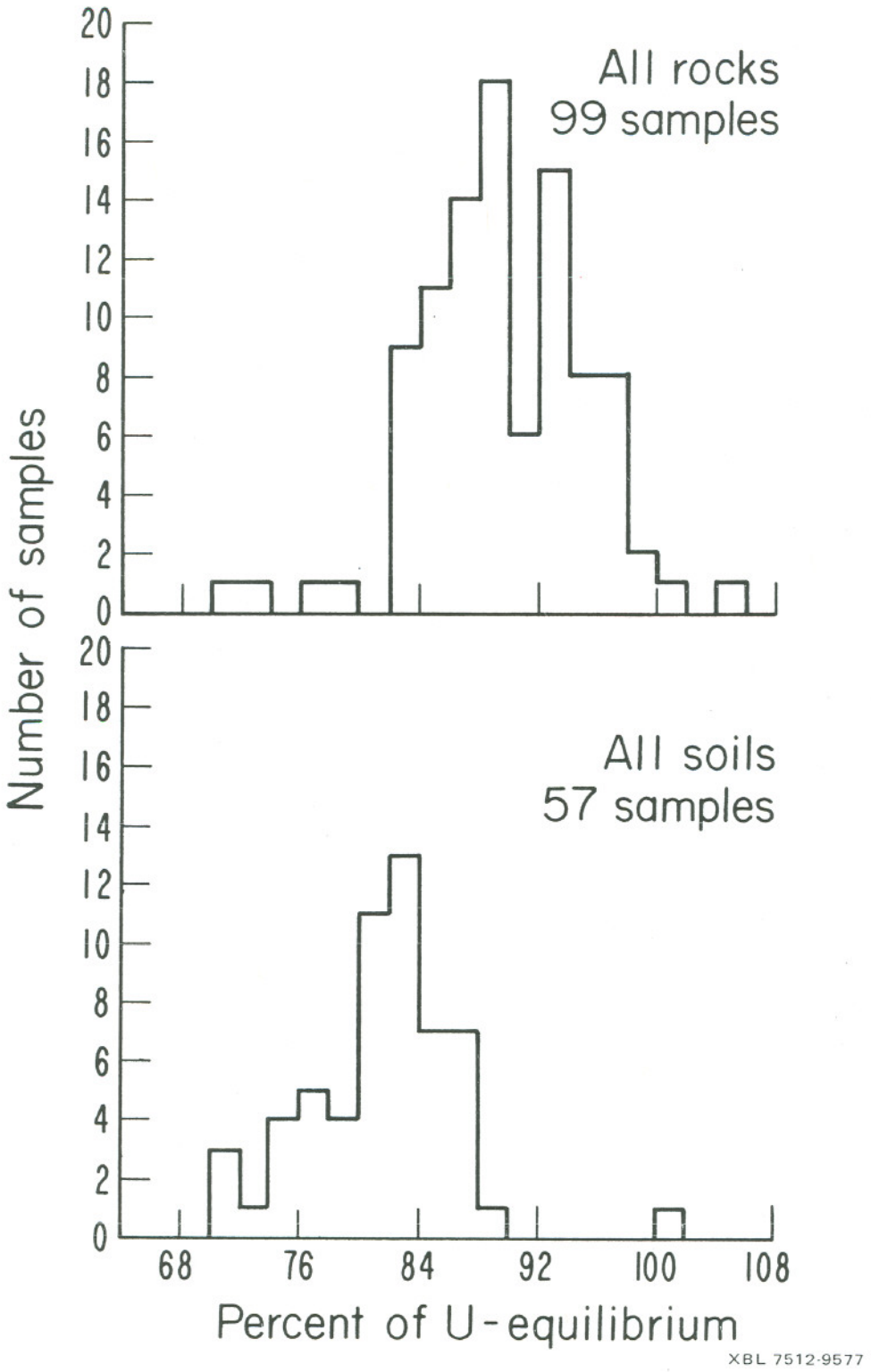

Fig. 5. Percent of U-equilibrium for all rock and all soil samples.

cherts, have high concentrations of uranium but low concentrations of thorium and potassium. These cherts occur only to a minor extent within the Laboratory boundary.

Because of the two distinct rock groupings there are two distinct dose rate distributions both from rocks and soils. Both the low activity rocks (Claremont, Orinda, and Moraga Formations) and the high activity rocks (Chico Formation) show log-normal dose rate frequency distributions as may be seen from an inspection of Figs. 6 and 7.

From these data dose rates ranging from 1.7 to 12.3 μr/hr are inferred from the rock samples and dose rates ranging from 1.9 to 9.9 μr/hr are inferred from the soil samples. Thus exposure rates on the LBL site may vary by more than a factor of two within a distance of less than 10 meters. Variations of greater magnitude may be observed, even in undisturbed regions, indicating the difficulty in determining background dose rates due to natural radioactivity to better than 10 millirem/yr.

The difficulty in obtaining an accurate value for the dose rate from natural radioactivity is increased by secular variations in background at a given location, which are due to four predominant causes, listed in order of importance as follows:

1. Soil moisture content (0.5-2.5 μrem/hr)
2. Decay series disequilibrium (0.1-0.5 μrem/hr)
3. Nuclear weapons fallout (<0.2 μrem/hr)
4. Atmospheric Rn-222 concentration (∿1 μrem/hr)

Burke[8] has studied the temporal variations in natural background at several locations in New York and New Jersey. She attributes the

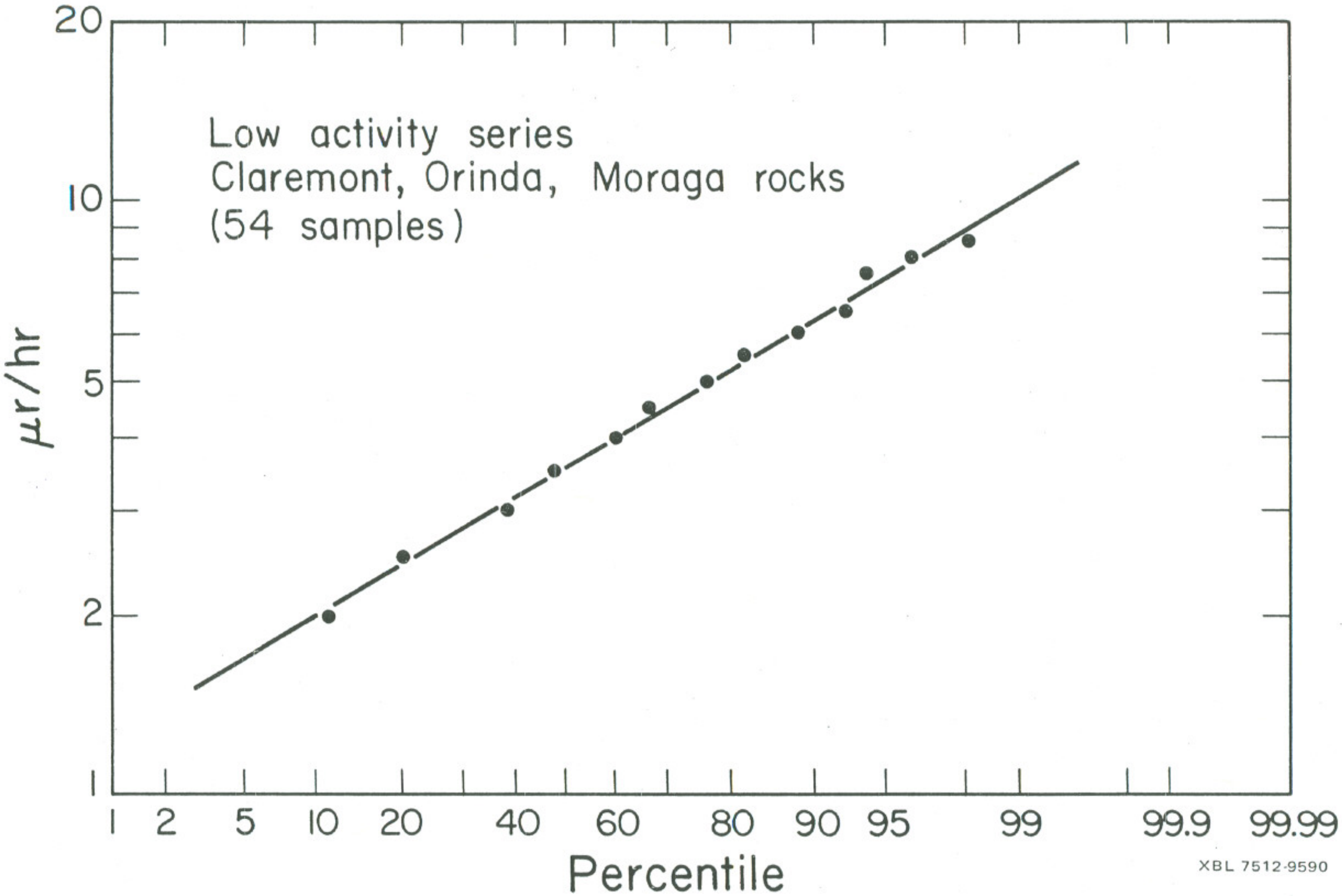

Fig. 6. Log-normal distribution of all low activity series rock samples.

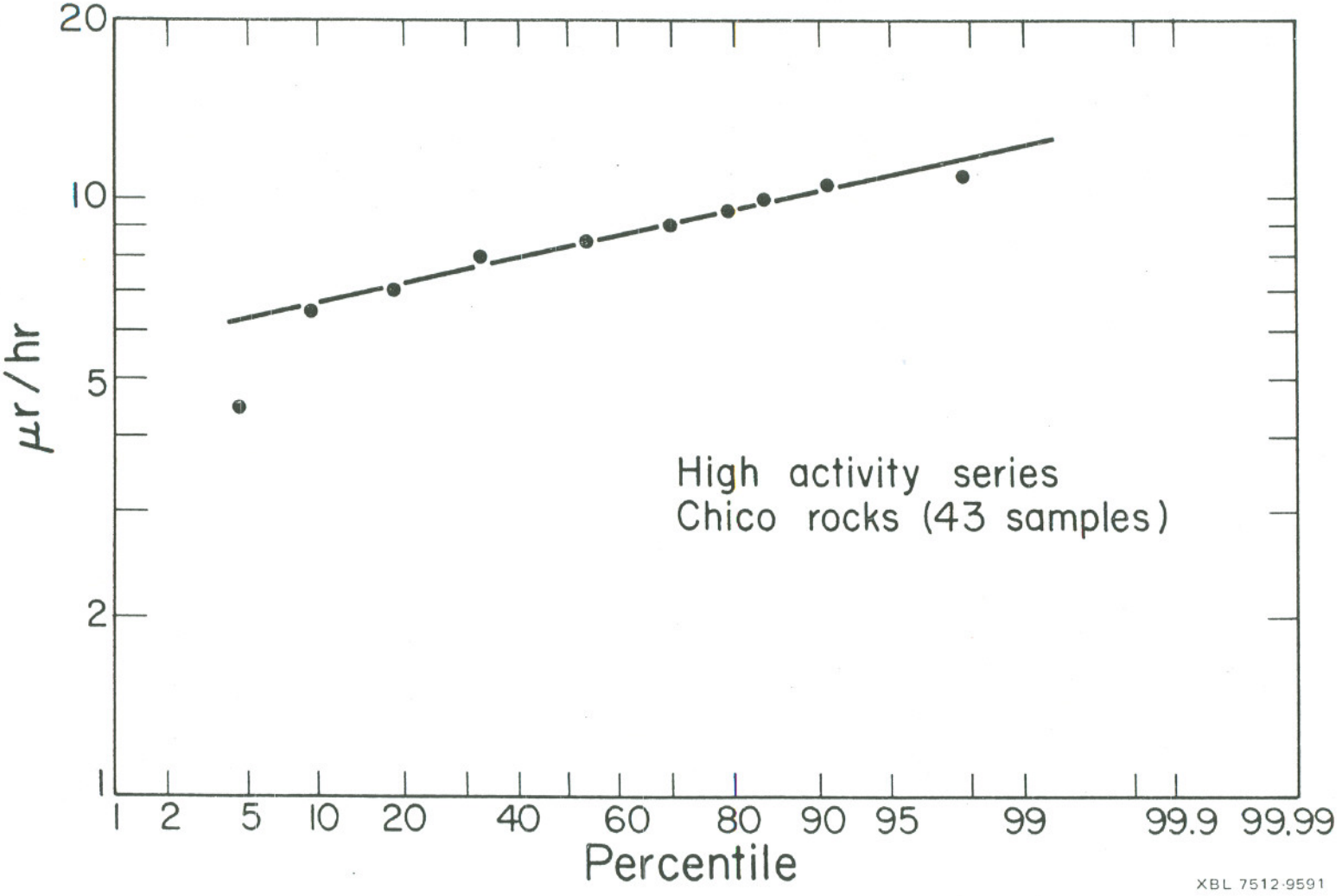

Fig. 7. Log-normal distribution of the high activity Chico formation rock samples.

observed fluctuation primarily due to changes in the density of the soil-water medium and to standing water or snow cover on the ground surface.[9] Soils on the LBL site exhibit the full range of moisture content, from zero to saturated, each year. These changes would result in changes in the dose equivalent rates from about 0.6 to 2.8 μrem/hr. Detailed studies of this source of variations have not been made at LBL because our accelerators operate almost continuously. By selecting those brief periods when all accelerators are not in use, data on radiation levels at different periods are being accumulated.

Values of dose rate calculated from the known composition of rock and soil will give an upper limit which assumes that all the decay-chain radionuclides in the earth have achieved secular equilibrium. In general this is not so because radon and thoron are able to diffuse from the rock or earth into the atmosphere. Measurements of the degree of uranium on the LBL site have been made. Rocks showed an average 89% U-equilibrium condition, while soils averaged 82% U-equilibrium. All the samples tested, but one, showed some degree of disequilibrium (See Fig. 5). Thorium series disequilibrium does not significantly reduce the observed dose rate because of the short half life of thoron (54 secs).

The degree of U-series disequilibrium observed indicates that the greatest decrease to be observed in the field would be 5% below that inferred from laboratory analysis of field samples. The range of intensity changes due to disequilibrium are from 0.1 to 0.5 μrem/hr (about 1 to 5 millirem/yr).

The degree to which nuclear weapons fallout influences γ- ray background will depend upon the exact location. At the present time it may amount to an exposure rate of $\sim$0.2 μr/hr in the San Francisco Bay Area, but it may contribute much less.[10] These levels, which are largely determined by ^{137}Cs which has a half life of 30 years, will not change rapidly with time in the absence of further weapons testing in the atmosphere.

Little is known about the contribution to dose rate from radon which has diffused into the atmosphere. Very large variations (more than two orders of magnitude) in the concentration of ^{222}Rn have been observed. Changes in ambient γ-ray exposure rates of 10-30% have been observed following rainfall which washes out dust particles to which radon daughters have become attached.

In the mid 1960's, atmospheric ^{222}Rn contents were measured in the Berkeley area by collecting air samples on activated charcoal and subsequently analyzing them by gamma-ray spectrometry for ^{214}Bi and ^{214}Pb.[11] Geographic location and atmospherics play the major role in determining the Rn content at a given site. Relatively low values were observed at the LBL site (17 to 65 pCi/m^3), and even lower contents measured at the shoreline of San Francisco bay, a few miles west of the site.

Most of these measurements were made when prevailing westerly or northwesterly winds were blowing; considerably greater values (hundreds of pCi/m^3) are to be expected during infrequent stagnant air conditions or on the rare occasions when winds blow from the east or northeast. Since the prevailing westerlies mainly traverse the

open ocean, they receive little radon, compared to easterly or northeasterly winds which have traversed the radon-emanating land mass. Stagnant air associated with a strong inversion allows accumulation of radon without appreciable dispersion, accounting for relatively high atmospheric content on such days. While much needs to be learned, it seems probable that changes in the concentration of atmospheric radon and its daughters can result in changes in exposure rate of up to ∿1 μr/hr.

In summary, the analytical approach to environmental radiation measurements described here is of great value. When field measurements of background γ-dose-rates are not possible because of continuous laboratory operation, it may be used to estimate long term integrals of natural background rates to an uncertainty of ∿30%, depending upon the particular conditions at the time of measurements. In some circumstances accuracy is limited by variations of soil moisture content (∿25%), uranium series disequilibrium (∿5%). Estimates of the contribution to ambient radiation levels due to fallout can be obtained from a laboratory assay of surface samples. Much more needs to be learned about the dose rates due to atmospheric radon and its daughters. In any case, detailed knowledge of the natural background will facilitate correct interpretation of any changes noted in environmental radiation levels.

1.4.3. Cosmic Radiation

The most important components of the radiation environment due to cosmic radiation at the bottom of the atmosphere are conveniently subdivided into the ionizing components and the neutron component.

1.4.3.1. Ionizing Component of the Cosmic Radiation. At sea level the most important part of the ionizing component of the cosmic radiation consists of muons (the "hard component") which are produced by the decay of pions high in the atmosphere. The only other component of major importance is the electronic (or "soft") component produced by the decay or collision of the muons. The soft component contributes about 30% of the total intensity of the sea-level ionization.

The radiation levels due to the ionizing component of cosmic radiation at several locations in the United States have been determined by Beck et al. of the Health and Safety Laboratory, New York.[5] Measurements of the total ionization were made using steel-walled cylindrical ionization chambers filled with pure argon at a pressure of 1000 psi. This instrument responds to ionization produced by cosmic radiation, natural radioactivity, and nuclear weapons fallout. The contribution from the latter two sources was determined separately by in situ γ-spectrometry, using a NaI(Tl) detector. Ionization produced by the cosmic radiation was then inferred by subtraction. Greatest accuracy was obtained at locations where the natural radioactivity of the surrounding rocks was low, or on the surface of large lakes.

Measurements were made at seven sites in California, in collaboration with the Health Physics Department of the Lawrence Berkeley Laboratory, and the data obtained and summarized in Table 2.

The measurements at altitudes up to 1000 ft are of value in establishing the natural background component due to cosmic radiation at the Lawrence Berkeley Laboratory. Table 2 gives values of 3.6 μR/hr (sea level), 3.8 μR/hr (960 ft), 3.86 μR/hr (933 ft) with a mean value

Table 2. Cosmic Ray Ionization Measurements in California Made by the Health and Safety Laboratory.

Location	Date	Altitude (ft)	HASL Inferred Cosmic Ray Dose Rate μr/hr
Copperopolis, CA (Asbestos Mine)	8-28-65	933	3.86
Goleta Beach, CA (Sand Beach)	8-31-65	Sea Level	3.6
Linda Loma, CA (School Lawn)	8-31-65	960	3.8

of 3.75 μR/hr. Of these three measurements, the one taken at Copperopolis (3.86 μR/hr) is probably the most accurate, since the natural radioactivity of the surrounding serpentine rock was extremely low. Taking this value, the annual exposure rate is 33.8 milliroentgens/yr, and the corresponding dose equivalent is 32 millirem/yr.

1.4.3.2. Cosmic Ray Produced Neutrons. At sea level, neutrons contribute about 10% of the total radiation exposure to man from cosmic rays.[12] Neutrons reaching the Earth's surface are principally created in the Earth's atmosphere by the interaction of the primary cosmic rays with oxygen and nitrogen nuclei at high altitudes and in the subsequent development of a hadronic cascade down through the atmosphere. Two nuclear reactions are important in the production of cosmic-ray neutrons: direct inelastic reactions producing "knock-on" neutrons, with energies from about 1 MeV to well in excess of 1 GeV, and evaporation processes in which neutrons peaked around 1 MeV are emitted in the de-excitation of nuclei following inelastic processes.[12]

The atmospheric neutron intensity depends on the intensity of charged particles reaching the atmosphere, which in turn depends on the strength of the Earth's magnetic field. Consequently, the neutron flux density increases with geomagnetic latitude because charged particles of lower momentum may enter the atmosphere.

At sea level, the neutron flux density is small and difficult to measure since it is easily perturbed by local terrain. Table 3 summarizes some of the more recent data and shows differences of nearly a factor of 3. Estimates of the sea-level intensity from

Table 3. Summary of Sea-Level Cosmic-Ray Neutron Data.

References	Latitude, Deg	Neutron Flux Density, $n\text{-}cm^{-2}sec^{-1}$
17	41	0.01
14	46	0.0065
18	46	0.0180[a]
19	55	0.0180[b]
13	46	0.0084
15	44	0.0074
16	41	0.0082

[a]Obtained by Watt et al.[19] extrapolating higher altitude data to sea level using 145 g/cm^2 relaxation length.

[b]Average value from the results of several investigators as extrapolated.

measurements at higher altitudes assuming an exponential variation with pressure altitude are extremely sensitive to the value of attenuation length assumed. If such extrapolated estimates are not considered, the recent measurements by Kent,[13] Boella et al.,[14] Yamashita et al.,[15] and Hajnal et al.[16] agree to within about 30% ranging from 6.5×10^{-3} to 8.4×10^{-3} $n\text{-}cm^{-2}sec^{-1}$. These differences may be due to variation with time of the neutron flux density and the influence of the air-earth interface on the measurements. The measurements of Yamashita et al. were made at Berkeley and showed that near the earth-air interface there is an enhancement in the mean thermal energy component of the spectrum because of increased production, moderation and backscattering.

Interpretation of the neutron flux density measurements in terms of dose-equivalent rate requires knowledge of the neutron spectrum. In 1959, Hess et al.[12] reported one of the first measurements of the energy spectrum of cosmic-ray neutrons in the energy region between 0.01 eV and 10 GeV at several altitudes. One significant feature of their spectrum is a peak at a few MeV, attributed by the authors to nuclear evaporation processes. Only a few measurements of neutron spectra have been reported since then, and the most recent do not extend over as wide an energy range as that of Hess et al. The most recent measurement comparable with that of Hess et al. was done by Hajnal et al.[16] using Bonner spheres. These measurements show general agreement with the spectrum derived by Hess et al. Work is continuing at the Lawrence Berkeley Laboratory to improve measurements of the cosmic ray produced neutron spectrum using activation detectors and Bonner spheres.[20]

Shaw et al.[21] have derived fluence to dose-equivalent factors for neutron spectra and for the Hess cosmic ray spectrum obtained a value of 1.3×10^{-8} rem $n^{-1}cm^{2}$. Combining this factor with a mean neutron flux density of 8.0×10^{-3} n $cm^{-2}sec^{-1}$, the annual dose-equivalent rate at sea level can be calculated to be 3.3 millirem/yr.

1.4.4. Nuclear Weapons Fallout

Since 1958 Lawrence Berkeley Laboratory has made measurements of external radiation levels at 30 locations in the San Francisco Bay Area.[22,23] The primary purpose of these measurements was to determine the magnitude of the external radiation levels due to nuclear weapons fallout. Measurements have been made in the field of total γ-exposure

rates using a portable 3 in.×3 in. NaI(Tl) scintillator counter and soil samples taken from each measurement site have been radio-assayed in the Laboratory. When fall-out levels are low, good agreement is obtained between calculated exposure-rate from the radio-assay data and measurements made in the field.

Since the cessation of nuclear weapons testing in the atmosphere, external radiation levels due to fall-out have declined and now amount to ∿0.2 μR/hr or less.

1.5. Climate and Meteorology

The general climate of a region has an influence on the background radiation levels due to natural causes (Section 1.4) and the meteorological conditions play a dominant role in the dispersion of any pollutants released to the atmosphere. Some general understanding of climate and meteorological conditions is, therefore, necessary to facilitate interpretation of data obtained by the Laboratory's environmental surveillance program (described in Section 3).

1.5.1. Climate

1.5.1.1. General Description. The Laboratory site shares the general climatic conditions of the Bay Region with some modification due to its hill side location at 400 to 1000 ft elevation overlooking San Francisco Bay to the west. The climatological summary for Oakland, where the nearest National Weather Service (NOAA) station is located, is also descriptive of Berkeley and is excerpted here:

"The climate of Oakland has three outstanding features: mild year-round temperatures; copious rains during the winter; and low overcast, clearing by noon and almost no rain during the summer.

"Located on the east shore of San Francisco Bay, Oakland enjoys a climate more equable than would be expected if latitude only were considered. Because of the prevailing westerly winds from the Pacific, where temperature varies very little between winter and summer, winters are mild and summers are cool. On an average of about 4 days a year, when northesterly winds have overcome the prevailing westerly wind, daytime temperatures may reach into the 90's, and on rare occasions (six times since 1928) temperatures of 100° or higher have been recorded. . . .during the winter normal daily minimum temperatures average 39.8° and on about 6 days temperatures of 32° or below can be expected. . .

"About 90% of the annual total rainfall is received in the 6 months, November through April. . . In spite of the almost rainless summers, however, cooling sea breezes, morning overcast, and rather high relative humidity prevent any semblance of a desert climate."[24]

1.5.1.2. Temperatures. The range between minimum and maximum temperatures at the Laboratory is greater than at the Oakland National Weather Service Station (which is situated at sea level) because of

the higher elevation of the Laboratory. The monthly temperatures for Berkeley are given in Table 4. The highest temperature ever recorded at the weather station on the University campus was 106°. Although normally freezing temperatures are encountered only a few days per year, occasional unusual cold spells have occurred, and these have sometimes caused significant damage to plants and to plumbing. The lowest temperature ever recorded in the area was 14° at the Botanical Garden, which is at the southwest edge of the Laboratory, during a period described as the Big Freeze of the Century." During this same period, the lowest temperature recorded at the Oakland Weather station was 26°.

1.5.1.3. Precipitation. A 16-year record maintained at the Laboratory indicates that 96% of the annual rainfall occurs during the months October through April. The average annual rainfall is 24.7 in., the wettest month being January, and the driest being August. Intensities seldom exceed 0.5 in. per hour or 2.5 in. during a 24-hr period. The most severe recorded rainstorm occurred in October 1962, when 13.90 in. fell during a 4-day period. On the average, there are 16 days a year with rainfall of 0.5 in. or more.[25]

Hail occurs rarely and has not been recorded to have been of damaging intensity. A trace of snow falls on an average of one day every 5 years; total snowfall at Berkeley has been less than 3 in. since 1900. There is an average of 3 thunderstorms per year. Average precipitation by months is given in Table 5.

Table 4. Berkeley Temperature (in °F) by Months, Measured on the Campus of the University of California.

	Berkeley Temperature, by Month, in Degrees Fahrenheit											
	Months											
	Jan.	Feb.	Mar.	Apr.	May	June	July	Aug.	Sept.	Oct.	Nov.	Dec.
Extreme High	77.0	80.0	87.0	91.0	91.0	101.0	97.0	92.0	106.0	99.0	86.0	76.0
Mean High	55.3	58.5	61.1	63.9	66.0	69.4	69.5	69.1	71.2	69.2	63.3	56.7
Mean	48.5	51.2	53.2	55.4	57.8	60.9	61.4	61.4	62.6	60.5	55.5	50.0
Mean Low	42.2	44.6	48.8	47.7	49.9	52.4	53.7	54.1	54.5	52.3	47.9	43.6
Extreme Low	28.0	29.0	34.0	36.0	36.0	42.0	42.0	46.0	46.0	39.0	33.0	30.0

Table 5. Monthly Precipitation at the Lawrence Berkeley Laboratory (in Inches). 17 years, 1958-75.

	Months											
	July	Aug.	Sept.	Oct.	Nov.	Dec.	Jan.	Feb.	Mar.	April	May	June
Maximum	1.59	0.57	3.34	14.33	11.17	8.86	11.65	10.49	6.93	6.44	1.79	1.14
Mean	0.10	0.06	0.41	1.76	3.78	3.95	5.51	3.56	3.19	1.95	0.24	0.20
Mimimum	0.00	0.00	0.00	0.03	0.00	0.58	1.61	0.16	0.43	0.01	0.00	0.00

1.5.2. Meteorology

1.5.2.1. Wind. A 5-year study of wind direction and speed collected by an anemometer located on top of Building 70 at the Laboratory gives a good indication of wind conditions to be expected. These data were averaged over 1-hr periods.[26] Table 6 gives the percentages of time that the wind blows from various directions and speeds. These frequencies are also depicted by wind roses in Fig. 8.

The 5-year wind study showed that

- No winds averaging over 27 knots in 1 hr were recorded.
- The most prevalent winds are westerly at 4 to 10 knots. (These occur 6.5% for all hours, 15.5% from 1600 to 1900).
- The strongest winds are usually from the southeast (SSE) at 11 to 21 knots, occurring during periods of precipitation (usually cyclonic storms moving in from the Pacific during the winter rainy season).

1.5.2.2. Inversions. The San Francisco Bay Area is a large shallow basin ringed by hills. Temperature inversions are frequent in the Bay Region, occurring about 2 out of every 3 days of the year.[27] These inversion layers act as barriers to the upward dilution of pollutants emitted within or below them. When the base of the inversion is below the elevation of the surrounding hills, and breezes are light, a stagnant air mass is formed, and "smoggy days" often result.

About 40% of the time the Laboratory, at its elevation of 400 to 1,000 ft, is either within an inversion layer, or below one whose base is under 2,000 ft, the elevation of nearby hills.[28] Either of these conditions results in impaired dilution and dispersion of any pollutant released from our site. Also, of course, during these periods the naturally occurring isotopes of Radon and their daughters

accumulate to concentrations several times higher than when atmospheric ventilation is more efficient.

Table 6. Distribution of Wind Direction and Speed, Averaged over 1 hr periods at the Lawrence Berkeley Laboratory (Frequency Given in Percentages).*

Direction	Speed (knots) 1-3	4-10	11-21	22-27	Over 27
N	0.59	0.97	0.05	0.00	0.0
NNE	0.61	0.61	0.01	0.00	0.0
NE	0.89	1.10	0.20	0.00	0.0
ENE	1.10	1.52	0.59	0.03	0.0
E	1.97	1.68	0.45	0.03	0.0
ESE	2.46	1.87	0.17	0.00	0.0
SE	3.31	3.53	0.39	0.01	0.0
SSE	3.59	4.67	1.13	0.01	0.0
S	3.12	4.44	0.70	0.01	0.0
SSW	3.36	3.86	0.18	0.00	0.0
SW	3.24	3.30	0.03	0.00	0.0
WSW	3.17	4.28	0.09	0.00	0.0
W	4.02	6.45	0.14	0.00	0.0
WNW	3.65	4.86	0.26	0.00	0.0
NW	3.33	3.19	0.13	0.00	0.0
NNW	1.64	2.24	0.08	0.00	0.0
Totals** (all directions)	40.05	48.66	4.60	0.09	0.0

* Based on 40,705 observations taken over a 5-year period.

** Wind was calm for 6.58% of the time.

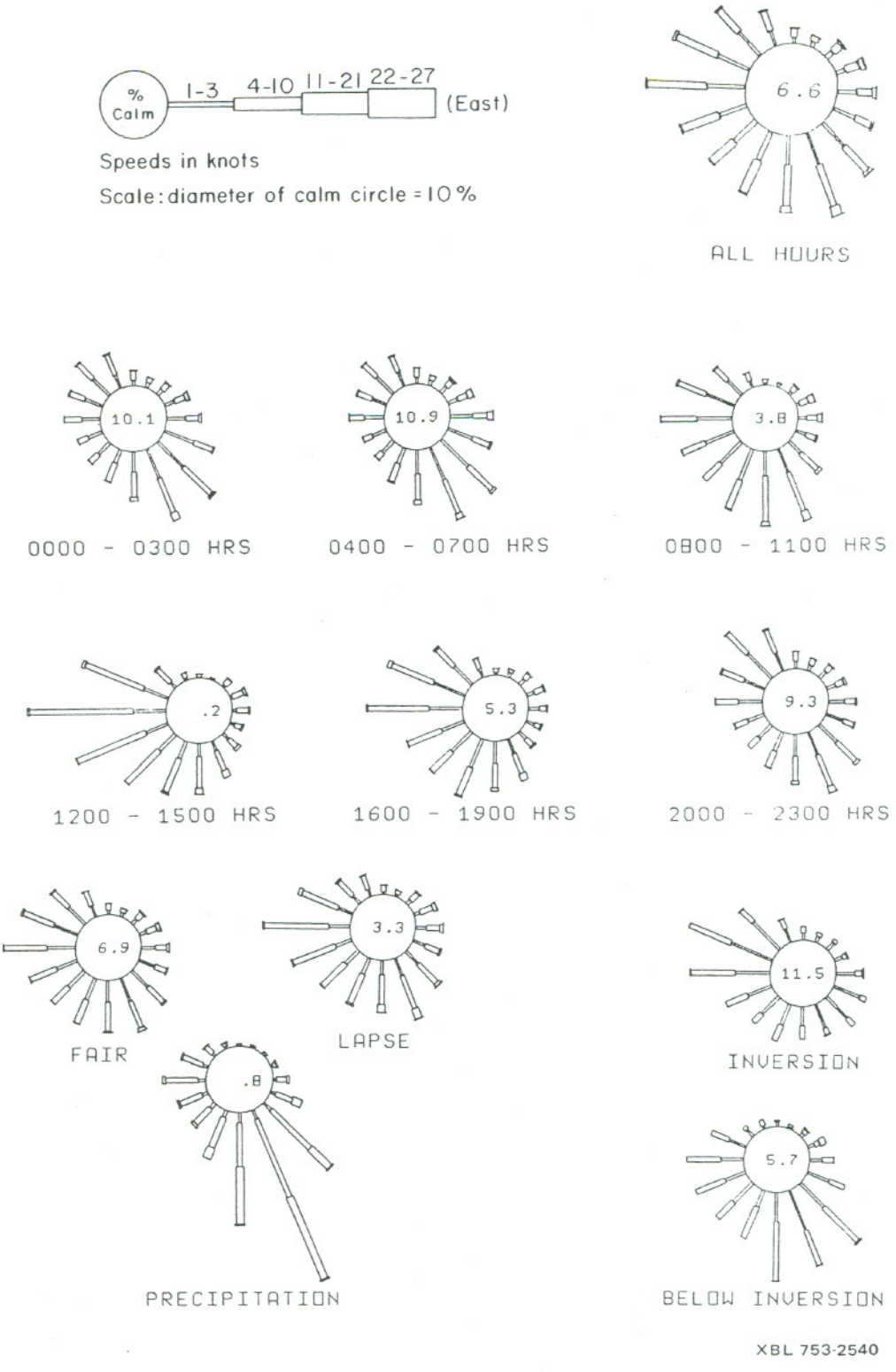

Fig. 8. Wind roses for LBL site, showing a) percent of time wind is calm (figure in circles) and b) percent of time (relative length in diameters) wind in speed ranges given in legend is from various directions.

2. The Potential Environmental Impact of the Lawrence Berkeley Laboratory

2.1. General

The potential environmental impact of the Laboratory may conveniently be divided into two categories of radiological and nonradiological. The radiological impact may be further subdivided into two subcategories, the first being the possible release of radionuclides to the environment and the second being the "prompt" radiation environment of photons and neutrons produced during accelerator operations. It is this latter sub-category that presents the largest potential source of environmental impact resulting from operations at the Lawrence Berkeley Laboratory.

2.2. Accelerator Radiation Environments (General)

The principal radiological impact on the natural radiation environment caused by the Lawrence Berkeley Laboratory is due to the operation of several particle accelerators, which are briefly described in Section 1.1. Two distinct and separate radiation fields are associated with particle accelerators. The first may be described as "prompt" and is directly associated with the operation of the accelerator. All components of this prompt radiation field disappear almost immediately upon accelerator turn-off, but it is this prompt radiation field that is the dominant source of radiological impact on the environment. The second radiation field may be described as "remanent", since it remains after accelerator operation has ceased; it is due to radioactivity induced in the accelerator components, shielding, and surrounding environment. This remanent radiation

field is usually of no environmental consequence. Thus the environmental impact of high-energy accelerators is different in character from most types of nuclear installations. At accelerators the predominant source of population exposure is from the radiation field produced during operation rather than from the leakage of radionuclides into the environment.

The environmental impact of the prompt and remanent radiation fields is discussed in some detail in the next two sections.

2.2.1. Accelerator Produced Penetrating Radiation--the "Prompt" Radiation Field

Use of accelerators in high-energy research inevitably leads to the production of many new and unfamiliar radiation environments which require investigation. The "prompt" radiation fields of particle accelerators are potentially extremely complex, particularly at the highest energies when many rare and unusual particles can be created. All particles produced by high-energy accelerators occur in nature, as a result of interactions of the galactic cosmic radiation, but their rate of production is extremely small. One of the primary motives for the development of high-energy accelerators was to increase the production rate of such rare particles so that their physical properties could be studied. The relatively low production rate of such particles, however, means that they play an unimportant role in determining the character of particle accelerator radiation environments, which, experience has shown, are dominated in most practical situations by photons (γ-rays) and neutrons.

Since the late 1940's extensive experience has been obtained at Berkeley of the radiation environment of a variety of accelerators, including the various cyclotrons, a proton synchrotron, a proton linac, electron linacs, an electron synchrotron, and a heavy ion linac. A significant fraction of the present understanding of accelerator radiation phenomena directly derives from studies made at LBL.[29-31]

Much of the past effort of the Health Physics Department has been directed to the development of an analytical technique of radiation monitoring by which the various components of a radiation field are identified. The intensity and energy distribution of those particles which are present in significant quantities are then determined. From these energy spectra the dose equivalent is calculated. Such an approach has the advantage that sufficient information is obtained to implement many aspects of a health physics program--the anticipation and prior estimation of radiation intensities, their measurement and field estimation, and the design of shielding and operational procedures which ensure adequate safeguards but permit experimental flexibility.

The work of the group in radiation detector development and shielding measurements has been extensively described in the literature--most recently condensed in several review articles.[32,34] From this work a general rule has emerged. Outside of high energy accelerator shielding, neutrons between 0.1 and 20 MeV usually contribute more than half the total dose equivalent. Gamma-rays and low-energy neutrons together contribute 10-20%, with neutrons greater than 20 MeV making up the balance. In the past few years it

has become possible to measure the neutron energy spectrum, which exists outside accelerator shielding, with adequate detail for radiation protection purposes.[33] Such studies show that, with the exception of the SuperHILAC, the radiation environment outside the shielding of the LBL accelerators is dominated by neutrons.

The Bevatron, when accelerating protons, is a significant source of neutrons. It has been estimated that, with an internal beam intensity of 3×10^{12} protons per pulse, the effective source strength of the roof shielding is between 1 and 3×10^{9} neutrons sec^{-1},[35] while with an extracted beam intensity of $\sim6\times10^{11}$ protons per pulse, $\sim2\times10^{8}$ neutrons sec^{-1} leak from the experimental area shielding.[35]

Under certain operating conditions as many as $\sim10^{9}$ neutrons sec^{-1} leak from the shielding of the 184 in. synchrocyclotron.

In the immediate vicinity of the SuperHILAC, X-rays dominate the radiation levels along the prestripper and poststripper tanks of the linear accelerator. The production mechanisms of these photons are not fully understood and is currently being investigated. It is known that the bremsstrahlung intensity is independent of heavy ion beam intensity but increases rapidly with voltage gradient along the accelerator. Attenuation measurements show that the photon energies are about 1 MeV.

Neutrons are also produced by the SuperHILAC and measurements at the Laboratory's environmental monitoring stations show that, when averaged over periods of several months, photons and neutrons contribute about equally to the dose equivalent produced by the SuperHILAC at the Laboratory's perimeter.

The character of the leakage neutron spectrum from the shield of these accelerators is controlled by the interaction of neutrons of energy greater than about 100 MeV. The nature of the equilibrium achieved between these high-energy neutrons and their interaction products is determined by the nuclear properties of the shield. The most commonly used shielding material is concrete whose nuclear properties do not differ greatly from those of air. The equilibrium spectra established in these two media, therefore, do not differ greatly.

Measurements of the spectrum of neutrons emerging from the Bevatron shield show it to be qualitatively similar to the energy spectrum that is produced by the interaction of cosmic radiation with the atmosphere.[12,33] There are some quantitative differences, however; the dose equivalent per unit fluence for neutrons emerging from the Bevatron shielding is a factor of about 1.5 greater than that for the cosmic ray neutron spectrum.[21] The neutron leakage spectrum from the 184-Inch Synchrocyclotron is assumed to be similar to that from the Bevatron. The neutron spectrum from the 88-Inch Cyclotron and the SuperHILAC will be much "softer" since the maximum neutron energy that may be produced by these accelerators is very much lower. Under some operating conditions, any one of these accelerators may have a stray radiation field which can be detected as a small addition to the neutral background radiation at distances as great as a few thousand feet. This small increased radiation intensity at a given location and time may consist of contributions from any or all of the accelerators. The energy of the neutrons

leaking from the accelerator shield determines how they are transported through the atmosphere. Measurements within the Lawrence Berkeley Laboratory show a reduction of neutron dose equivalent with increasing distance from both the 184 in. Cyclotron and the Bevatron.[36] Examples of such measurements made around the Bevatron are shown in Fig. 9. Neutron dose equivalent is diminished by geometrical dilution (inverse square law) and by absorption in the atmosphere. Many measurements of the variation of dose equivalent as a function of distance from accelerators have been published in the literature, and critically reviewed in a recent article[37] (see also Sect. 4.2.1.).

2.2.2. The Production of Radionuclides in the Environment by High Energy Accelerators

As we have seen (Sect. 2.2), the production of radionuclides in the environment by accelerator operation is potentially a much smaller source of population exposure than the "prompt" penetrating radiation.

Possible contamination of the ground water close to accelerator laboratories and consequent contamination of drinking water has been carefully studied at the Stanford Linear Accelerator 20-GeV electron linac,[38,39] the 24-GeV proton synchrotron at CERN,[40,41] the 400-GeV proton synchrotron at the National Accelerator Laboratory,[42] and elsewhere.[43-47]

General consideration of the total quantity of radionuclides produced in the earth shields of high-energy accelerators suggests no serious contamination problems in volumes of water comparable to rainfall on the accelerator site.[48] Such studies all conclude that no significant ground water contamination is likely due to accelerator operation. This conclusion has been supported to date by the absence

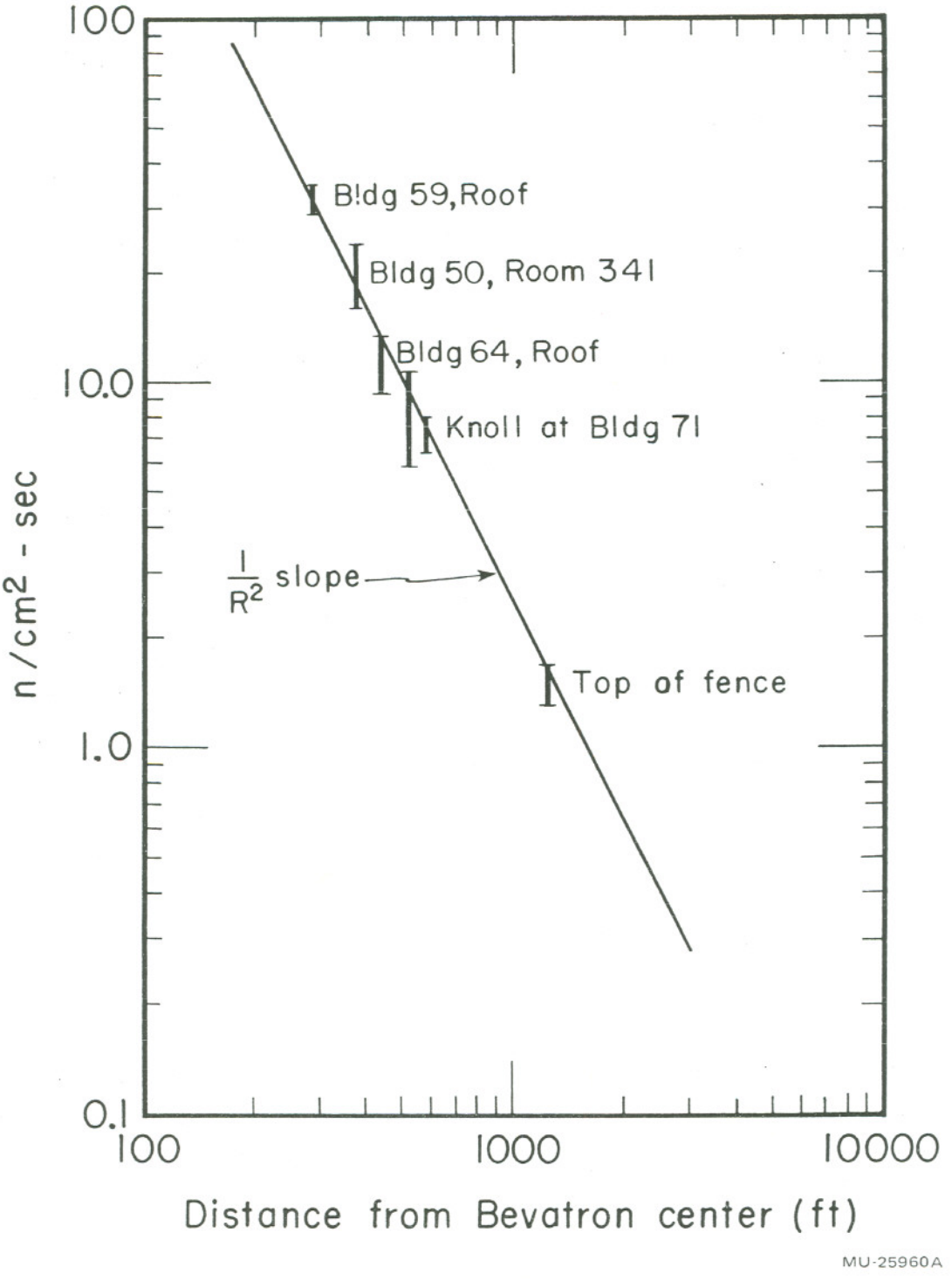

Fig. 9. Measurement of neutron flux density around the Bevatron.

of any reports in the literature of any significant elevation in the radioactivity in water supplies close to accelerator laboratories.

Long experience with the operation of diverse types of particle accelerators makes it possible to conclude that the exposures resulting from radioactive gases or aerosols produced by particle accelerators are usually significantly lower than those due to the external radiation field. Measurements of the production of radioactive gases have been reported[49-58] and show that in many cases in the immediate vicinity of high energy particle beams the air may be extremely radioactive. Most of the radionuclides are, however, extremely short-lived and do not survive in significant concentrations outside accelerator installations. ^{3}H and ^{7}Be are two examples of long-lived radionuclides of significance. Recent studies have been made at CERN as part of the design studies for a 300-GeV proton synchrotron[59] and the 600-MeV synchrocyclotron improvement program.[60] The CERN studies conclude that despite the high beam power of the new accelerators under construction, external radiation due to accelerator operation will continue to predominate. Calculations show that the concentration of ^{7}Be deposited on neighboring vegetation will be comparable to that produced by the interaction of cosmic radiation with the atmosphere, and will barely be detectable. Preliminary studies by Smith[61] of the ^{7}Be concentration on vegetation and gravel around the Lawrence Berkeley Laboratory and its vicinity do not indicate any measureable production of ^{7}Be that may be attributed to accelerator operation. Measurements of ^{3}H around high energy accelerators have not been reported but similar conclusions are to be expected.

No radionuclides due to the operation of high energy accelerators at LBL have been detected in the environment.

2.3. Leakage of Radionuclides into the Environment from Chemical Laboratories

The use of radionuclides in the various research laboratories is the principal potential source of leakage of radionuclides into the environment. Both air and water might potentially be polluted, but this potential is minimized by Laboratory policy which requires that research using quantities of radioactive materials, which if released could result in a concentration greater than 1% of the radiation protection standard off site, are confined to glove boxes which exhaust through high efficiency particulate air (HEPA) filters. No releases of radionuclides either to surface streams or to the sanitary sewer are permitted.

Studies of the various pathways by which radionuclides might be discharged from the Laboratory and measurements of the concentrations of radionuclides in the pathways permits close control at possible locations where radioactive materials might be released. Every chemical laboratory room has its own locally controlled exhaust system, discharging individually into the atmosphere. Over 100 such exhaust points exist, located on a number of different buildings throughout the site, all of which are sampled and analyzed to determine the quantity of radioactive material released. This policy has had the desired result and releases which could result in concentrations greater than 1% of the pertinent radiation protection standard seldom, if ever, occur.

All liquid waste known to be radioactive is collected, solidified, and shipped away. Other liquid wastes are discharged directly into the municipal sewer system. There are two outfalls, each of which is monitored by a continuous sampling system, to ensure that no significant quantities have been discharged accidentially.

The storm drainage from the Laboratory flows into the surface streams which discharge into San Francisco Bay. For the most part, these streams travel in underground conduits but are exposed as they run through the University property and are sampled in three places (see Sect. 3).

2.4. Non-Radiological Environmental Impact

2.4.1. Air Pollution

The principal potential source of air pollution is due to combustion devices. All stationary heating devices at the Laboratory utilize clean-burning natural gas (propane is sometimes used in emergencies). The combustion processes used at the Laboratory do not generate pollutants (e.g., SO_2, CO, hydrocarbons, photochemical oxidants, nitrogen oxides, particulate matter) in quantities sufficient to warrant constant monitoring.

A small workshop utilized in the machining of beryllium is a potential source of air pollution, but all machines are totally enclosed and vented through high efficiency air filters. In view of the rigorous controls over all aspects of the operation of the beryllium shop, the Environmental Protection Agency has granted a waiver for the need to carry out environmental monitoring for beryllium.

2.4.2. Water Pollution

No Laboratory wastes are discharged to the two surface streams which run through the Laboratory site (Blackberry Canyon Creek, Strawberry Canyon Creek, see Fig. 10). All effluent from Laboratory processes, cooling towers, and industrial processes is discharged to the municipal sanitary sewers. The regional sanitary sewer works finds no unacceptable pollutants in Laboratory wastes.

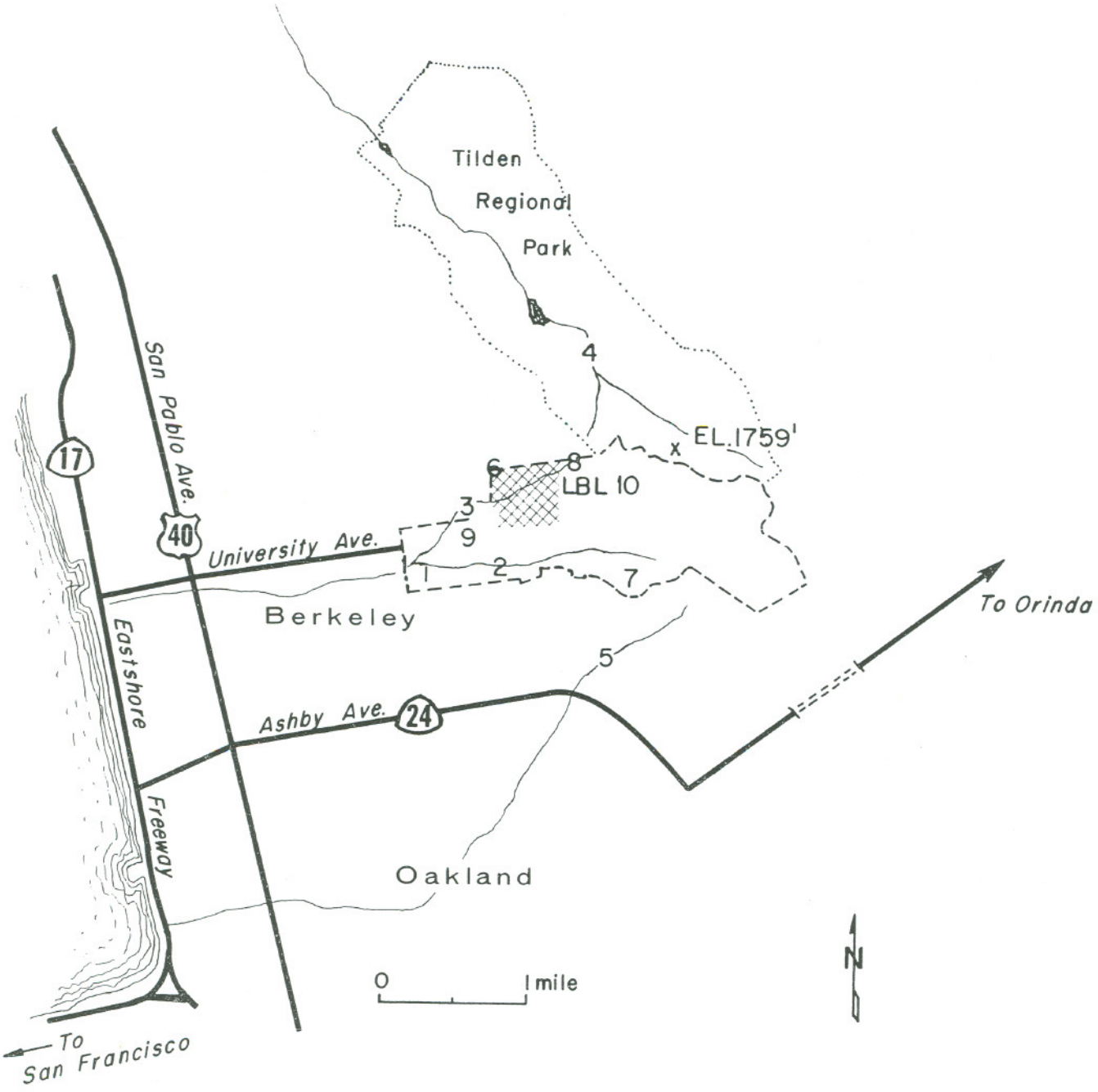

Fig. 10. Plan of the University of California Campus and the Lawrence Berkeley Laboratory, showing their relation to the cities of Berkeley and Oakland.

3. The Environmental Surveillance Program of the Lawrence Berkeley Laboratory

3.1. Environmental Monitoring of Accelerator-Produced "Prompt" Radiation

Estimates of the contribution dose equivalent at the Laboratory boundary due to accelerator operation have been made for many years. Records show that since estimates have been made,[62] levels at the site boundary have been consistently below the maximum permissible dose-equivalent for non-occupational exposure recommended by the ICRP.[63] It should be explained that the values of dose equivalent reported represent an upper limit and--as we shall show later--may in fact have been substantially lower. When there has been some uncertainty in the interpretation of site boundary radiation measurements, it has always been policy at the Lawrence Berkeley Laboratory to report the more conservative (higher value). Over the years, increasing knowledge of accelerator radiation phenomena has permitted us to report site boundary radiation levels with greater accuracy.

Estimates of the small contribution to the total dose equivalent, made at the Laboratory boundary by the operations of our accelerators, have been made continuously for many years. An analytic method is used to monitor the various components of the accelerator-produced radiation field. From the particle fluence and measured energy spectrum, the dose equivalent is calculated. The environmental radiation monitoring system now in use at the Lawrence Berkeley Laboratory makes possible continuous measurements and permanent records of both the rate and the time-integrated intensity of radiation exposure. It also provides a means for rapid determination

of the relative contributions of each of the several accelerators to the total radiation environment by making use of accelerator maintenance shutdown periods during which radiation levels at remote locations are studied under different combinations of accelerator operating conditions.

Since 1964 radiation levels at ten locations have been continuously monitored, as shown in Fig. 11.[64] These locations were strategically selected to monitor the radiation output of the Laboratory's accelerators, both close to each accelerator and to the Laboratory perimeter. Four stations are used to monitor radiation levels within the accelerator buildings, giving an indication of accelerator operating conditions. One station (which was taken out of service in 1972) was used to monitor radiation levels in downtown Berkeley. Two environmental monitoring stations (situated at the Olympus Gate and adjacent to the 88-Inch Cyclotron) are specifically located to record the highest radiation levels at the Laboratory boundaries, while two others--those at Building 90 and at Panoramic Way--respond to skyshine from the Bevatron and the 88-Inch Cyclotron and to direct radiation from the 184-Inch Cyclotron, respectively. The signals from each of these environmental monitoring stations are telemetered to the Health Physics laboratories in Building 72.

3.1.1. Instrumentation in the Environmental Monitoring Stations

At each station gamma ray exposure levels are measured with an energy-compensated Geiger-Muller counter of the type designed by Jones.[65] The complete radiation detector assembly consists of a thin window GM tube in a stainless steel cylinder and the associated

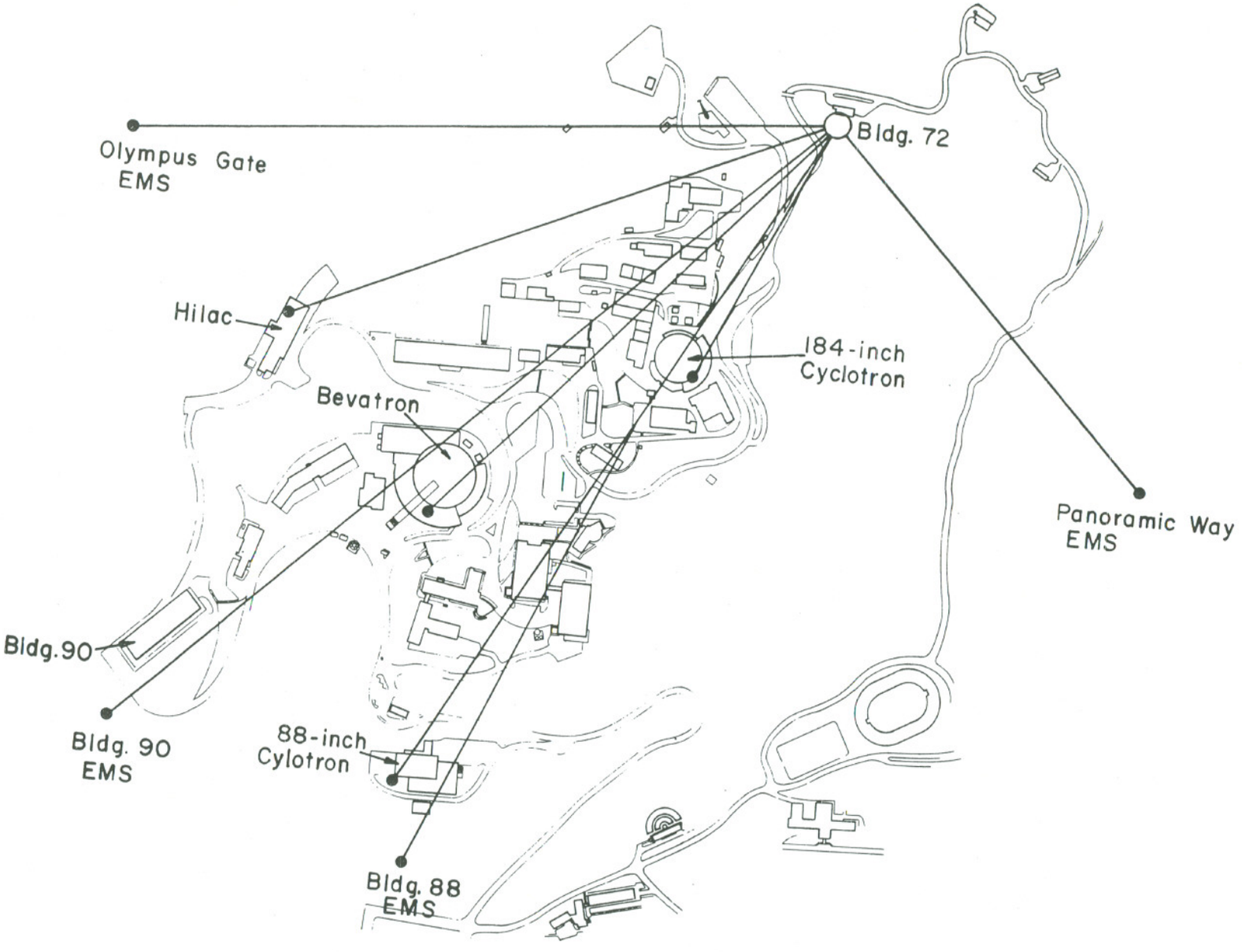

XBL 677-3568

Fig. 11. Plan view of the Laboratory showing the location of the environmental monitoring stations.

transistorized circuitry and scaler units. Each dosimeter is packaged in a metal box 6 in.×6 in.×9 in., with the GM tube assembly, 6 in.×1-1/2 in., mounted on top of the box. The units, while normally ac powered, also contain a rechargeable battery which will run the detector for ∿6 weeks, in the event of an ac power outage. The detector and scaler unit are designed to obtain a sensitivity of ∿1 microroentgen per register integer. Each Geiger-Muller unit is calibrated with an NBS standard 1.35 milligram radium source, and the average sensitivity is 1.8 μR per register count.

The primary neutron detector at each station is a BF_3 gas proportional counter in a 2-1/2 in.-thick paraffin-lined moderator. This detector is sensitive to neutrons whose energies lie in the range from 0.1 to 20 MeV.[66] From time to time other neutron detectors such as a bismuth fission chamber[67] are operated at the monitoring stations to determine high-energy neutron fluences.

3.1.2. Natural Background at the LBL Environmental Monitoring Stations

Field measurements of the component of natural background due to terrestrial radioactivity have been made with a portable NaI(Tl) counter in the vicinities of the four permanent monitoring stations. One set of data was taken in December 1973 during a period when laboratory operations were shut down for the holidays, thus enabling us to measure environmental radiation levels free from possible effects of accelerator operation. A second set of measurements was made in mid-summer 1974.

Portable instrument readings were taken at a number of locations within a circular area about 30 ft in diameter centered on each station, to determine variations in gamma-field intensity within the area sampled by the station detector, and also to provide control for composite soil samples concurrently taken from within the same area. Measurements were also taken inside each station house at the site of the integrating GM detector and were lower than those outside because of two factors. Firstly, the radioactivity of the materials used to construct the station was lower than that of earth, and secondly, the station itself provided some shielding from external radiation.

The San Francisco Bay Region has two seasons--a dry season which runs from April until October, when rainfall is sparse, and a wet season from October until the end of March, when intermittent storms produce considerable rainfall (see Sect. 1.5).

Thus, the December measurements were taken at a time when soil moisture content was approximately at maximum. Soil moisture acts as a shielding material (water) that is interspersed with the source material (soil); hence, greater soil moisture produces lower gamma-intensity. The December data thus represent minimum values for the ambient natural gamma-ray field. Since the soil is more nearly dry on an annual <u>average</u> basis, data taken in the summer of 1974 during the dry season provides a closer estimate of the average ambient gamma-field intensity; these data are listed in the third column of Table 7, and provide the best present estimate of the annual <u>natural</u> gamma-dose integral at the LBL environmental monitoring stations.

Table 7. Background Gamma Radiation Levels Measured at the LBL Environmental Monitoring Stations. (For Locations of Stations, see Fig. 10).

Environmental Monitoring Station	Soil Condition/Measurement Location		
	Wet/Outside (mR/yr)	Wet/Inside (mR/yr)	Dry/Inside (mR/yr)
Building 88	57	46	59
Building 90	44	37	51
Olympus Gate	32	26	36
Panoramic Gate	50	39	62

In addition to the background radiation from terrestrial radioactivity listed in the third column of Table 7 must be added 32 millirem per year from ionization produced by cosmic rays and 3.3 millirem per year from cosmic ray produced neutrons (Sects. 1.4.2 and 1.4.3) to give the total annual background rate.

3.1.3. Analysis of the Data Obtained from the Environmental Monitoring Program

In general, the response of each monitoring station is a complex function of the mode of operation of each and all the Laboratory's accelerators. Without more detailed studies than have so far been made it is not yet possible to accurately assign the relative contributions to the radiation level at each station to particular accelerators. By studying the radiation level at each station to particular accelerators. By studying the response of each environmental station to the various conditions of accelerator operation, however, it is possible to derive a general understanding of the response of each environmental monitoring station. The trends of radiation levels

observed at the various monitoring stations and correlations with accelerator operation are discussed in annual environmental monitoring reports published by the Laboratory and have been reviewed by Thomas.[68]

The maximum permissible annual dose equivalent to which members of the general population may be exposed (at the boundary of a laboratory such as Lawrence Berkeley Laboratory) is 500 millirem/yr. It has been Laboratory policy to place considerable effort on maintaining radiation levels well below this limit. In fact, in recent years the radiation levels on the Laboratory boundary due to accelerator operation have been comparable with the fluctuations in radiation intensity which occur in nature; therefore, there is inevitably some uncertainty in the values of dose equivalent reported by our environmental monitoring system.

This uncertainty does not reflect the accuracy of the physical data obtained from the monitoring program--but rather the uncertainty in converting this data to units of dose equivalent for the purposes of radiation protection. The ICRU has recognized this difficulty, and suggested that when the maximum dose equivalent is considerably less than the radiation protection standard, an uncertainty of as much as a factor of three in estimation of the dose equivalent is acceptable.[69] However, much greater accuracy is often demanded in the reporting of environmental data.

The difficulties which result from fluctuations in γ-ray background at a particular location have already been discussed (Sect. 1.4.2). An accuracy of better than 20 millirem/yr for the γ-ray background is

difficult unless expensive and sophisticated techniques, such as continuous γ-ray spectrometry, are used.[70,71]

The determination of neutron dose equivalent also presents some problems. Neutrons up to an energy of 20 MeV may be readily measured with a moderated BF_3 counter, and the neutron fluences at the site boundary in this energy region may be determined with good accuracy. Conversion of this fluence to dose equivalent is, however, a more difficult matter.

The evaluation of dose equivalent consists of two steps: a physical measurement capable of good accuracy, and the conversion of this physical measurement to units appropriate to radiation protection. This is limited by a general lack of knowledge in radiobiology. The assignment of the appropriate conversion factor is, to some extent, an arbitrary matter. It is, in essence, an administrative judgment. The problem is compounded by the fact that the accelerator-produced neutrons are distributed over a wide range of energy, and neutrons greater than 20 MeV in energy may make a significant contribution to the dose equivalent.

Although the ICRP have published fluence to dose equivalent conversion factors for monoenergetic neutrons,[72] there is no official guidance as to how such factors should be used for neutrons distributed in a continuous energy spectrum. The relative numbers of high energy (greater than 20 MeV) to low energy neutrons in a spectrum can greatly influence the biological potency of the overall neutron fluence. For example, the biological potency of neutrons in the cosmic ray spectrum is lower than that of neutrons emerging from the shielding of the Bevatron by a factor of 1.5.[73]

For neutron spectra, the dose equivalent at the maximum of the dose equivalent-depth distribution in the body should be used to calculate fluence-dose equivalent conversion factors.[16,21] Shaw et al.[21] have reported calculations of the conversion factors for a variety of spectra, both for unilateral and multilateral irradiation which are summarized in Table 8. Conversion factors for multilateral irradiation are used in the conversion of neutron fluence to dose equivalent for the environmental monitoring data.

Table 8. Dose Equivalent Per Unit Fluence for Cosmic Ray and Bevatron Shield Leakage Neutron Spectra (from Shaw et al.).

Neutron Spectrum	Dose Equivalent Per Unit Fluence (rem $n^{-1}cm^2$)	
	Unilateral Irradiation	Multilateral Irradiation
Cosmic Ray (Hess et al.)	1.97×10^{-8}	1.27×10^{-8}
Bevatron	2.33×10^{-8}	1.86×10^{-8}

3.2. Monitoring of Radionuclide Releases

3.2.1. Atmospheric Sampling

Every chemical laboratory room has its own locally controlled exhaust system, discharging into the atmosphere. There are over 100 such exhaust points, located on a number of different buildings throughout the site, and each is sampled and analyzed to determine the quantity of radioactive material released.

In addition to the monitoring of air from exhaust stacks, several air-sampling stations are situated throughout the Laboratory and at the Laboratory primeter. These environmental stations serve

three purposes. Firstly, they establish the general levels of the radioactivity of particulates in the air in the vicinity of the Laboratory; secondly, should any radionuclides be released from the Laboratory, the actual concentrations at the site perimeter would be determined. For this reason the location of some air samplers is chosen to be in the direction of populated areas from the Laboratory (see Fig. 10). Thirdly, should a significant accidental release occur, the sampling program provides direct measurements from which population dose equivalent estimates may be made. Because these quantities are very small, in general, only the gross α- and β-activities are determined. The lower limits for detection by the techniques used are 0.002 pCi Ci/m^3 for alpha emitters and 0.08 pCi Ci/m^3 for beta emitters. (For a summary of sampling methods and techniques of analysis, see Table 9).

In addition to gross α and β-activity measurements, tritium and ^{14}C are monitored by special samples taken in the areas potentially most susceptible to significant releases.[28]

Atmospheric deposition of radionuclides is determined at each of the environmental monitoring stations (Sect. 3.1). Rain or dry fallout is collected in 15-in. diameter containers. If no rain has fallen the containers are rinsed out with distilled water to obtain a sample.

3.2.2. Water Sampling

All liquid wastes known to be radioactive are collected, solidified and shipped from the Laboratory. Other liquid wastes are discharged directly into the municipal sewer via two outfalls, each of which is

continuously monitored to ensure that no significant quantities of radio-nuclides have been discharged. No wastes are discharged to the surface streams which run through the Laboratory site. Weekly water samples are taken from five locations to ensure that no accidental releases of radionuclides have occurred (see Fig. 10, Table 9).

The storm drainage from the Laboratory flows into surface streams which ultimately discharge into San Francisco Bay. For the most part these streams travel in underground conduits, but are exposed as they run through the University and are sampled at three places (see Fig. 10). To provide a basis for comparison, water from two nearby streams and incoming drinking water is also sampled.

Experience over many years has shown that the gross α and β activity measurements lie within the range of normal background. Therefore, alpha and gamma spectrometry are not routinely performed on water samples. However, γ spectrometry would be necessary in the event of significant release of accelerator-produced rationuclides.

Comtamination of the ground water from accelerator-produced radionuclides is a remote possibility (see Sect. 2.2.2). The appearance of unusual quantities of ^{3}H, ^{7}Be or ^{22}Na in the ground water might signal accelerator-produced contamination in the environment. These radionuclides are also cosmogenic, and it is therefore necessary to have some understanding of the naturally occurring levels of these radionuclides if emissions from accelerators are to be detected.[74,75] To date, detailed studies at LBL have been limited to ^{7}Be.

High energy particle accelerators produce ^{7}Be by the interaction of hadrons greater than about 30 MeV. The ^{7}Be produced in the accelerator

Table 9. Sampling Methods and Techniques of Analysis for Air and Water samples.

Air Samples (perimeter and on-site)	Four cfm through 4 in. 9 in. HV-70 paper. Sampling is continuous and the paper is changed weekly. 10 ml/min through silica gel and NaOH solution for HTO and $^{14}CO_2$.
Deposition Samples	Fifteen-inch diameter cylindrical container. Sample taken monthly. If there has been no rain the container is rinsed with 1 liter of distilled water.
Sewer Samples	Both sewers have continuous automatic samplers. Assays are made weekly. Sampling rates are 10 to 20 parts per million.
Surface Water and Tap Water	1 quart "grab" samples taken weekly.
Assay Methods	Air samples are counted directly with a thin-window large area flow counter for alpha activity and 30 mg/cm^2 GM tubes for beta activity. The limit of detection for alpha emitters is 0.002 pCi/m^3, and the limit for beta emitters is 0.08 pCi/m^3. HTO and $^{14}CO_2$ samples are assayed by methods described in Ref. 2. Detection limit: 0.7 and 0.2 nCi/m^3, respectively. Water Samples are evaporated into 2 in. planchets and counted for beta radiation in a low background thin-window GM flow counter and for alpha emitters in an internal-flow proportional counter. Sewer samples are run in duplicate, one being specially treated to retain halogens; the higher of the two counts is recorded. Limits of detection for these samples vary, depending on the solids content and the size of the sample assayed. Conditions are always chosen such that a concentration of 10 pCi/liter, either alpha or beta, can be detected.
Counting Efficiencies	With the "thick" samples involved, self absorption as well as absorption in counter windows is important. The counting efficiencies normally used are based on the assumption that alphas have 5.15 MeV and betas have 1 MeV.

structure and shield is tightly bound in the constituent materials and is not likely to migrate into the environment. ^{7}Be produced in closed water cooling systems can only be accidentally released. ^{7}Be produced in the atmosphere, either in airborne particulates or by interaction with the atmosphere may, however, escape the accelerator room and mix with the atmospheric reservoir appearing in the environment as "man-made" radioactivity.

The cosmogenic production rate of ^{7}Be production leads to an average deposition rate on the earth's surface of $\sim 10^{6}$ ^{7}Be atoms cm^{-2} per year. Allowing for radioactive decay and the 10% decay branching ratio for γ-emission, this deposition rate would give an equilibrium γ-ray activity of 3×10^{-3} $\gamma\, cm^{-2} sec^{-1}$. This surface activity gives rise to an exposure rate $\sim 2\times10^{-3}$ $\mu r\ hr^{-1}$, 1 meter above the surface--to be compared to exposure rates in the range 3-30 $\mu r\ hr^{-1}$ due to U, Th, K (Sect. 1.4.2). At this small exposure rate, the ^{7}Be contribution is masked by the competing radionuclides in field surveys--even when a Ge(Li) γ-spectrometer is used. It is, however, possible to detect ^{7}Be in the atmosphere and hydrosphere when the quantities of competing radionuclides are relatively low and concentration may enhance the ^{7}Be activity. Furthermore, the superficial ^{7}Be deposit may be measured by the laboratory assay of samples. This is easiest for rocks of low specific activity such as serpentine.

A measurement of the natural ^{7}Be deposition rate has been made at an uninhabited ultramafic ridge-top above Tiburon in Southern Marin County (some 10 miles northwest of LBL). Measurements of the activity of soil, serpentine fragments, and a single lichen-covered serpentine

slab gave an estimated ^{7}Be deposition rate of 0.77 pCi cm^{-2}--in reasonable agreement with the value of 0.68 pCi estimated by the uniform deposition model.

Figure 12 shows γ-spectra for two samples of low activity rocks taken from Marin and Alameda counties. The top curve (1) shows the spectrum for residual serpentine soil from a level area in Marin County. The second curve (2) shows the activity in serpentine debris washed down from a cut in serpentine rock onto a flat area. This sample was collected in the East Bay hills in February 1973 at a point some 6 miles from LBL. The ^{7}Be peak in the second curve is considerably enhanced over that shown in the first curve, suggesting concentration of ^{7}Be at this site. Such concentrations of ^{7}Be are frequently found in areas where ^{7}Be may be absorbed from rainwater falling in the locality. Concentration factors as high as two orders of magnitude are not uncommon. The third curve shows the decay of the second sample after 280 days; it may be seen that the ^{7}Be peak is substantially reduced. The fourth curve shows the background spectrum. Beyond the 2.6 MeV thorium series peak, the background and sample spectra are all identical.

Greater concentrations of ^{7}Be may be found in foliage; growing or dead leaves and grasses retain some of the atmospheric fallout, including ^{7}Be, that is deposited on their surfaces. The bracken fern, widely distributed in the Pacific States, is a convenient plant for fallout studies since the annually produced fronds have large horizontally arranged leaf area. It is possible to distinguish between dead fronds which are one or two seasons old, and it is

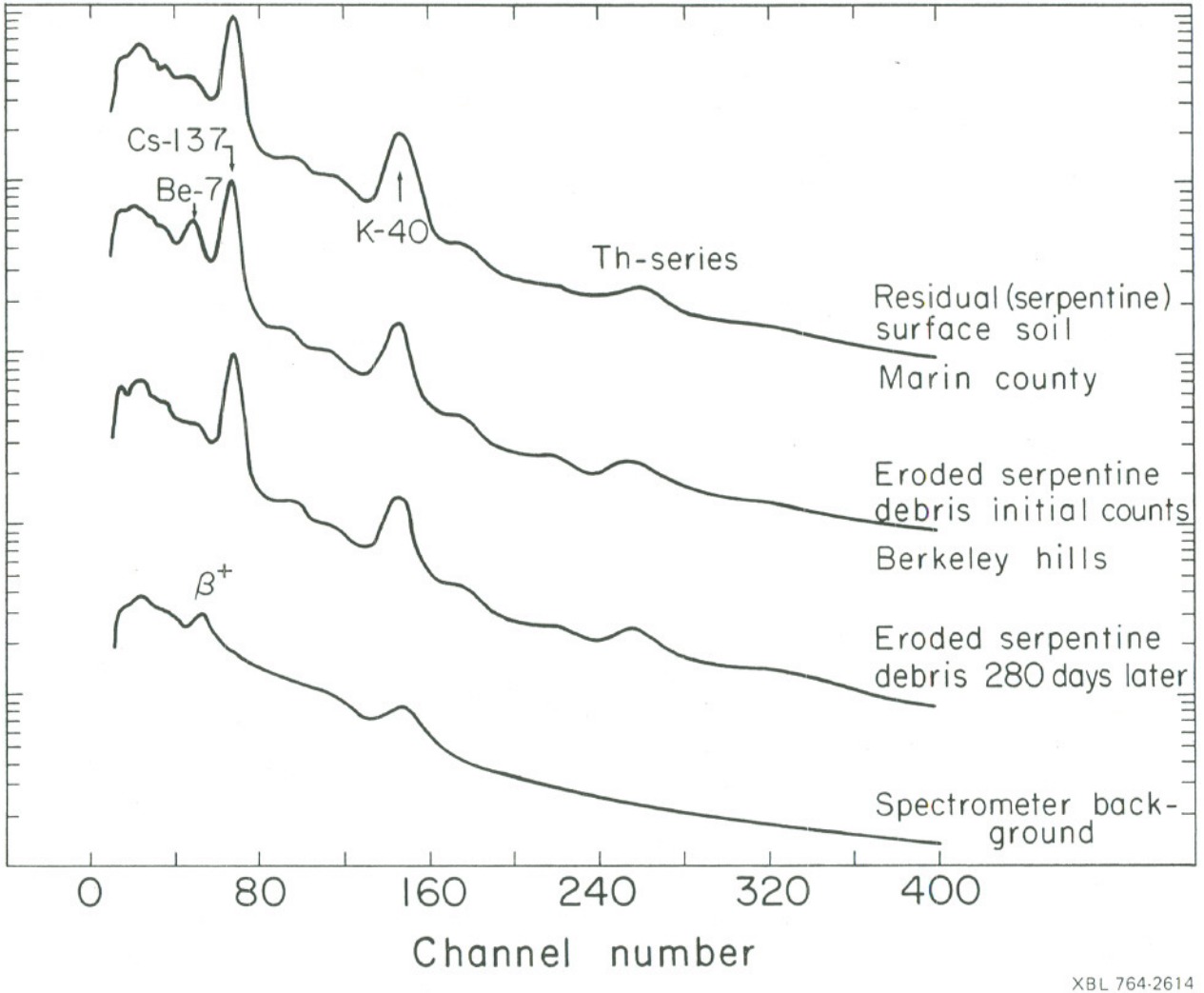

Fig. 12. Gamma-ray spectra of several samples taken from ultramafic terrains in Marin and Alameda counties.

therefore possible to collect samples of different age. Furthermore, braken grows either in open sunlight or in shade and studies of the influence of the overhead canopy of trees is possible. The collection matrix (cellulose) of the bracken is of extremely low radioactivity.

Bracken taken from a variety of sites in Northern California during 1973 have been radioassayed and these spectra are shown in Fig. 13. Table 10 summarizes the data; the ^{7}Be activity observed in the bracken ranges from 1.4 to 2.1 counts min^{-1} per gm of bracken with the exception of one sample which was taken at the Caldecott Tunnel (location No. 5) about 1 month after the last rains of the wet season. Correcting for radioactive decay of ^{7}Be brings the value in excellent agreement with the other data.

There has been no evidence that operation of the particle accelerators at LBL elevates the levels of ^{7}Be found in foliage, ground water or surface gravels, sands and rock at the Laboratory.

3.3. Non-Radiological Pollutants

Because the potential for air and water pollution from non-radiological sources is negligible (Sect. 2.4), no continuous monitoring for combustion products or beryllium in air is carried out. No wastes are discharged to surface waters within the Laboratory, eliminating the need for monitoring for non-radioactive pollutants. All wastes discharged through the municipal sanitary sewers are monitored by the sanitary sewer works.

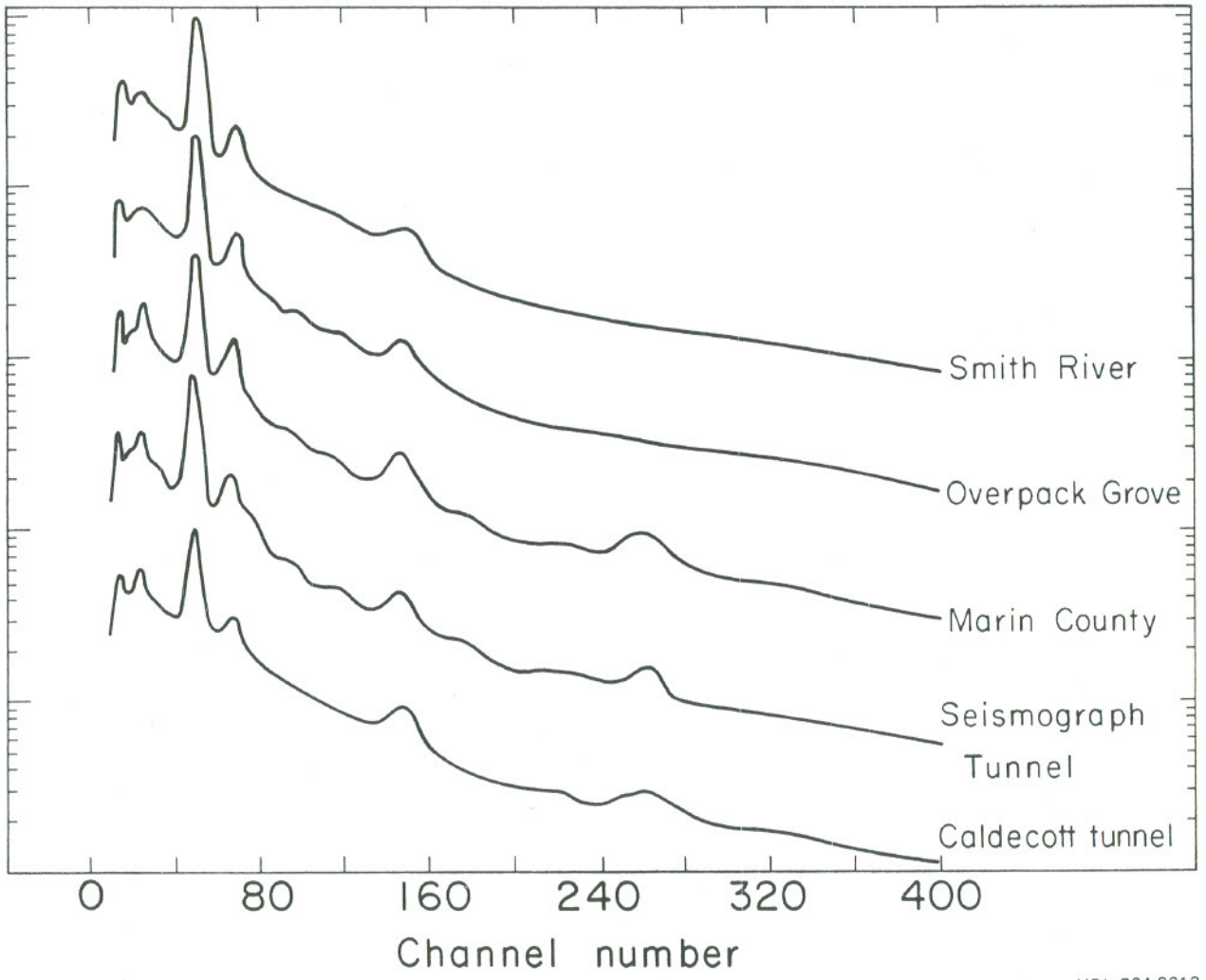

Fig. 13. Gamma-ray spectra of dried bracken samples collected during the 1972-1973 rainy season.

Table 10. Measurements of ^{7}Be in Samples of Bracken.

	Location	Collection Date	Specific Activity of ^{7}Be Counts min^{-1} cm^{-1} of Fern
1.	Smith River U.S. Route 199 ∿15 miles E of Crescent City 370 miles N of Berkeley	5/5/73	1.80
2.	Overpack Grove U.S. Route 101 Near Richardson's Grove ∿200 miles N of Berkeley	5/5/73	1.76
3.	Marin County, near Nicascio ∿30 miles NW of Berkeley	5/17/73	1.74
4.	University of California, Berkeley Seismograph Tunnel ∿1/2 mile S of LBL site on upper W-facing slope of Berkeley Hills	2/15/73	2.12
5.	Caldecott Tunnel State Route 24 ∿2 miles SE of LBL E side of Berkeley Hills	2/23/73 4/4/73 5/8/73	1.40 1.39 0.95*
6.	Santa Cruz Mountains ∿70 miles SW of LBL	1/26/73	1.71

*1.42 counts min^{-1} gm^{-1} when corrected for decay.

4. Models for the Calculation of the Population Dose Equivalent Due to LBL Operations

4.1. Introduction

As shown in Section 2, the major cause of radiation exposure to the general population as a result of LBL operations is due to the operation of four particle accelerators. Outside the Laboratory, these accelerators produce a small but measurable radiation intensity, largely consisting of neutrons. Such exposures are different, in some respects, from those at most nuclear installations and have consequently been studied in some detail.

In addition, the population may be exposed to small quantities of radionuclides released from the Laboratory. Typically, these exposures are considerably smaller (by more than an order of magnitude) than the population exposures resulting from accelerator operation and may be adequately calculated by techniques used at other nuclear facilities.

The population dose equivalent, M, is defined by the equation:[76]

$$M = \int H\, N(H)\, dH \qquad (1)$$

where N(H) dH is the number of people receiving a dose equivalent between H and H + dH.

Two different models for the estimation of dose equivalent have been developed for the two sources of population exposure.

4.2. Model for Estimating the Population Dose Equivalent Resulting from Accelerator Operation

In a homogeneous urban area, such as that surrounding the Laboratory, it is plausible that the population density at a given location may be considered constant when averaged over long periods of time.[77] This should not result in serious error in the estimate of population exposure, provided the intensity of accelerator operation is uncorrelated with fluctuations in population (e.g., high intensity operation is not restricted to times of known low population). If this assumption is made, Eq. (1) may be simplified to

$$M = \int_{r_0}^{R} H(r)\, N(r)\, dr \qquad (2)$$

where H(r) is the annual dose equivalent to a person at a distance from r to r + dr from the accelerator. The closest and farthest distances of approach to the accelerator are r_0 and R respectively. r_0 will correspond to the distance of the Laboratory boundary from the source of radiation. It is conventional to estimate population dose equivalent out to a distance of 80 kilometers from the facility, but, as we shall show later, in the case of the accelerator-produced radiation at Lawrence Berkeley Laboratory, essentially all the population exposure is contributed at distances less than 5 kilometers from the Laboratory.

Evaluation of the integral of Eq. (2) requires estimates of the distribution of population, N(r), and the variation of dose equivalent, H(r), with distance from the Laboratory.

4.2.1. Variation of Dose Equivalent with Distance from the Lawrence Berkeley Laboratory

Rindi and Thomas[34] have reviewed measurements of the variation of dose equivalent with distance made at many particle accelerators. Experimental data is limited to distances less than 1500 meters from an accelerator, but at all accelerators the dose equivalent beyond 300 meters falls faster than inversely, as the square of the distance from the accelerator. These authors conclude from the data that, in direct line of sight of shielded accelerators, the dose equivalent beyond 300 meters is probably best expressed in the empirical form:

$$H(r) = a \frac{e^{-r/\lambda}}{r^2} \qquad r \geq 300 \text{ meters} \qquad (3)$$

The parameter $e^{-r/\lambda}$ is attributed to air attenuation and λ may take the values between 225 and 850 meters. For accelerators capable of producing neutrons of energy greater than about 100 MeV, such as the 184-inch cyclotron and Bevatron, the higher value of λ should be used. Accelerators such as the SuperHILAC and 88-inch cyclotron do not produce neutrons greater than about 50 MeV in energy and, in this case, λ has a value of $\sim$250 meters.

4.2.2. Distribution of Population Around the Lawrence Berkeley Laboratory

The distribution of population around the Lawrence Berkeley Laboratory has been studied[78] using the U. S. Department of Commerce 1970 census data[79] and Campus statistics for the University of California

Berkeley Campus for 1972/73.[80] Figure 14 shows the regions investigated. Concentric circles at 1000 ft intervals were drawn around the Laboratory, between 1000 ft to 16,000 ft from the Bevatron. The residential population within each ring was obtained by summing the census data of the blocks located inside each circle. Table 11 summarizes the data so obtained.

The occupancy of the Campus of the University of California at Berkeley is not continuous. An estimate of the total time spent on campus by students is difficult in that non-instructional hours can vary widely with each student. Campus statistics for the University of California at Berkeley[80] show that a full-time-equivalent (FTE) student spends 450 hrs/yr in classroom instruction, but this will give a lower limit to the time spent on campus. An upper limit on campus attendance may be obtained from the University Catalogue which gives an FTE student as one that takes 36 units/year, each requiring 30 hrs of instruction and preparation (3 hrs/wk, 10 wk/quarter), giving a total of 1080 hrs/yr. Estimates of campus attendance for the average student may, therefore, range between 450 and 1080 hrs/yr, with an average of 765 hrs/yr, which is close to an earlier estimate of 780 hrs/yr given by Stephens and Thomas[81] (based on the assumption that students spend 4 hrs/yr, 5 days/wk for 39 wks/yr on campus).

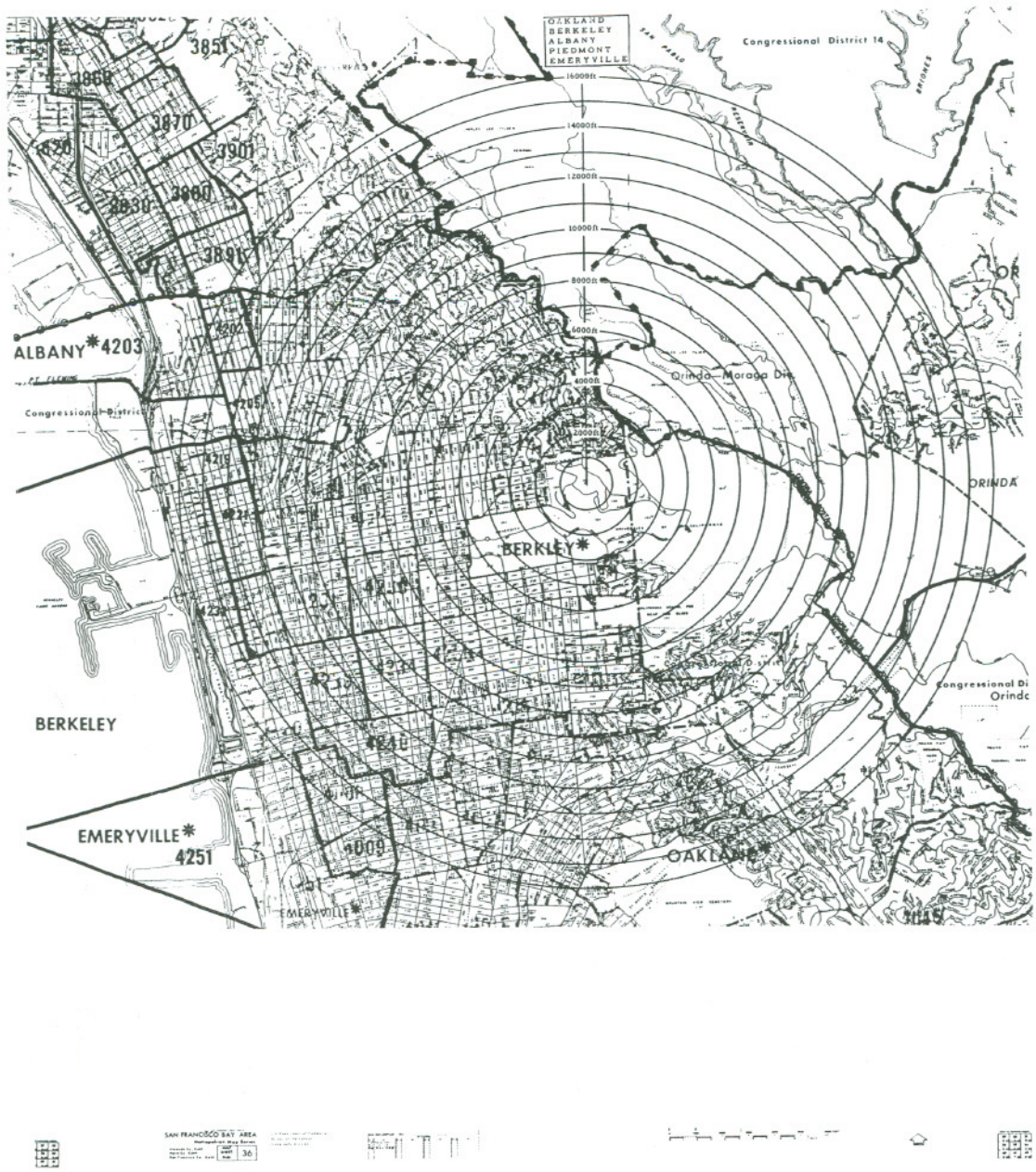

Fig. 14. Map of the area adjacent to the Lawrence Berkeley Laboratory.

Table 11 Distribution of population around the Lawrence Berkeley Laboratory

At distance(ft) from to	Residential population (Census data)	Average U.C. Berkeley FTER*	Total population
1,000-2,000	1,449	1,610	1,449
2,000-3,000	2,715	1,894	4,325
3,000-4,000	4,627	1,231	6,521
4,000-5,000	6,570		7,801
5,000-6,000	9,568		9,568
6,000-7,000	8,275		8,275
7,000-8,000	12,857		12,857
8,000-9,000	13,200		13,200
9,000-10,000	11,859		11,859
10,000-11,000	13.671		13,671
11,000-12,000	14,564		14,564
12,000-13,000	16,423		16,423
13,000-14,000	17,751		17,751
14,000-15,000	15,559		15,559
15,000-16,000	14,150		14,150
		Grand Total	167,973

*Full-time-equivalent resident.

In the data of Table 11 a value 765 hrs/yr has been taken in calculating the number of full time equivalent residents (FTER) on the University campus. In the 1973 report "Administration, Academic and Staff Personnel Headcount", the total FTE Berkeley staff numbered 9,809.[82] Assuming a full time employee works 40 hrs/wk for 46 weeks, staff and faculty contribute 2,059 FTER. From the residential population data and the estimates of University campus full time equivalent residents, the average population density in each ring shown on Fig. 14 may be calculated.

The use of these estimates of total population or population density in calculating population dose equivalent will give conservative (high) values for the following reasons:

a. Many students and staff members of the University of California, Berkeley, live close to the campus. They will, therefore, be counted twice in this estimate.

b. The daily migration of population to work places, stores, schools, etc, tends to be away from the Laboratory. Thus, for a significant fraction of the day the total residential population close to the Laboratory will be lower than that given in Table 11 .

From the data given in Table 11, values of N(r) may be obtained for the evaluation of the integral of Eq. (2).

4.2.3. Calculation of Population Dose Equivalent

Substitution of Eq. (3) into the expression for population dose equivalent gives

$$M = a \int_{r_0}^{R} N(r) \frac{e^{-r/\lambda}}{r^2} dr \tag{4}$$

where a has to be determined.

If the dose equivalent at distance r_0 from the Bevatron is H_0, substitution into Eq. (3) gives

$$a = r_0^2 H_0 e^{r_o/\lambda} \tag{5}$$

and Eq. (4) becomes:

$$M = r_0^2 H_0 e^{r_o/\lambda} \int_{r_0}^{R} N(r) \frac{e^{-r/\lambda}}{r^2} dr \tag{6}$$

The influence of the shielding of a large fraction of the population by the hills surrounding the Laboratory and by the buildings which it occupies may be included by writing:

$$M = \frac{r_0^2 H_0 e^{r_0/\lambda}}{S_1 S_2} \int_{r_0}^{R} N(r) \frac{e^{-r/\lambda}}{r^2} dr \tag{7}$$

where S_1, S_2 are shielding factors for the hills and buildings respectively.

The number of people N(r) between r and r + dr may be defined in terms of an average population density, $\sigma(r)$, defined by:

$$N(r) = 2\pi r \, \sigma(r) \, dr \tag{8}$$

and thus, finally:

$$M = \frac{2\pi\ r_0^2\ H_0\ e^{r_0/\lambda}}{S_1 S_2} \int_{r_0}^{R} \frac{\sigma(r)\ e^{-r/\lambda}}{r}\ dr \qquad (9)$$

When population density data are available in the form given in Table 11, it is convenient to approximate Eq. (9) by

$$M = \frac{2\pi\ r_0^2\ H_0\ e^{r_0/\lambda}}{S_1 S_2} \sum_{i=1}^{i=n} \sigma_i \int_{r_{i-1}}^{r_i} \frac{e^{-r/\lambda}}{r}\ dr \qquad (10)$$

where σ_i is defined by:

$$\sigma_i = \frac{N_i}{\pi\left(r_i^2 - r_{i-1}^2\right)} \qquad (11)$$

with N_i the number of people between r_{i-1} and r_i. The number of annuli, n, required for an accurate estimate of population dose equivalent is determined by the convergence properties of the integral in Eq. (10) and the upper limit of integration.

Population dose equivalent resulting from the operation of a nuclear installation is a scalar quantity, independent of distance from the installation, and the upper limit of the integral of Eq. (9) should, therefore, be infinity. The total population dose equivalent, M_∞, is then defined by:

$$M_\infty = \frac{2\pi\ r_0^2\ H_0\ e^{r_0/\lambda}}{S_1 S_2} \int_{r_0}^{\infty} \frac{\sigma(r)\ e^{-r/\lambda}}{r}\ dr \qquad (12)$$

Calculation of M from Eq. (9) will then result in a fraction, f, of the total dose equivalent, M_∞, defined by:

$$f = \frac{M}{M_\infty}$$

$$= \int_{r_0}^{R} \frac{\sigma(r)\ e^{-r/\lambda}}{r}\ dr \Big/ \int_{r_0}^{\infty} \frac{\sigma(r)\ e^{-r/\lambda}}{r}\ dr \qquad (13)$$

It is conventional to assume that the population dose equivalent has reached its convergent value ($M(R) = M_\infty$; $f = 1$) at a distance of 80 kilometers from a nuclear facility.

Studies have shown that the radiation exposure from accelerator operation at LBL, Eq. (12), converges extremely rapidly, having reached its ultimate value at about 5 kilometers from the Laboratory.[77]

Figure 15 shows the convergence of the calculated population dose equivalent for different values of neutron attenuation length in air, λ. Values of λ for the neutrons produced by the LBL accelerators lie between 225 and 850 meters (see Section 4.2.1). The data shown in Fig. 15 were calculated assuming a uniform population density distribution around the facility, but the results obtained also accurately describe the situation at the Lawrence Berkeley Laboratory.

Thus, in the numerical evaluation M from Eqs. (10) and (11) it was necessary to extend calculations out 5 km from and Lawrence Berkeley Laboratory and in the evaluation of the integral, the following values were used:

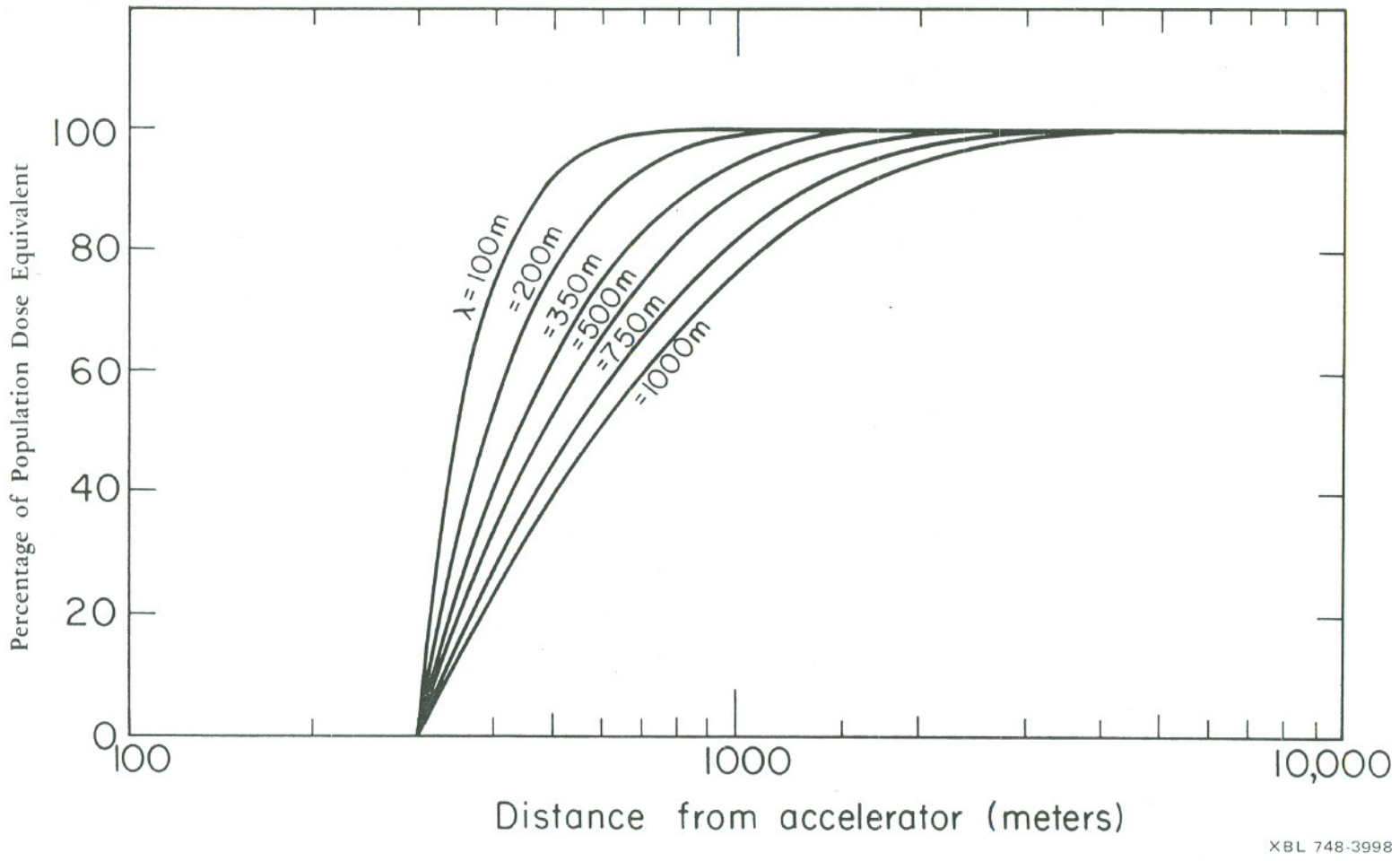

Fig. 15. The convergence of the population dose equivalent as a function of distance from the accelerator.

$$n = 0.15$$

$$r_0 = 366 \text{ meters (1200 ft)}$$

$$r_1 - r_0 = 244 \text{ meters (800 ft)}$$

$$r_i - r_{i-1} = 304.8 \text{ meters (1000 ft) for } r \geq 2$$

$$r_{15} = 4{,}877 \text{ meters (16,000 ft)}$$

$$\lambda = 850 \text{ meters}$$

$$S_1 S_2 = 2.2$$

Values of σ_i are given in Table 12. (Only approximate values of S_1 and S_2 are available.) Experimental data obtained by McCaslin[83] suggest that radiation levels are depressed by a factor of ~1.8 when hills intervene. Because most of the populated area is shielded by hills from a direct view of the dominant sources of accelerator produced radiation, we use a value of $S_1 \approx 1.8$.

Estimates for the shielding factor for buildings give a value of $S_2 \approx 1.2$ to the residential population and the students and staff of the University Campus.

A value of the product $S_1 S_2 = 2.2$ was used in these calculations. Substituting into Eq. (10) we obtain:

$$M/H_0 = 5.875 \times 10^5 \sum_{i=1}^{15} \sigma_i \int_{r_{i-1}}^{r_i} \frac{e^{-r/850}}{r} \, dr \quad . \qquad (14)$$

with r in meters, and σ_i in persons/m^2.[81] Values of the integrands of Eq. (14) were obtained by numerical integration and are summarized in Table 12. The population dose equivalent due to LBL accelerator operation calculated using this model is then:

$$M/H_0 \approx 1023 \text{ man rem/fence post rem} \quad .$$

Table 12. Evaluation of Population Dose Equivalent Resulting from Lawrence Berkeley Laboratory Accelerator Operation.

Distance (meters) From	To	σ_i (Persons/m^2)	I_i *	M_i/H_0 Man Rem/ Fence Post rem
366 (1,200 ft)	610 (2,000 ft)	$\sigma_1 = 1.94\times10^{-3}$	2.938×10^{-1}	341.1
610 (2,000 ft)	914 (3,000 ft)	$\sigma_2 = 2.96\times10^{-3}$	1.690×10^{-1}	299.2
914 (3,000 ft)	1219 (4,000 ft)	$\sigma_3 = 3.19\times10^{-3}$	8.343×10^{-2}	159.2
1219 (4,000 ft)	1524 (5,000 ft)	$\sigma_4 = 2.97\times10^{-3}$	4.511×10^{-2}	80.2
1524 (5,000 ft)	1829 (6,000 ft)	$\sigma_5 = 2.98\times10^{-3}$	2.571×10^{-2}	45.8
1829 (6,000 ft)	2134 (7,000 ft)	$\sigma_6 = 2.18\times10^{-3}$	1.517×10^{-2}	19.8
2134 (7,000 ft)	2438 (8,000 ft)	$\sigma_7 = 2194\times10^{-3}$	9.177×10^{-3}	16.1
2438 (8,000 ft)	2743 (9,000 ft)	$\sigma_8 = 2.66\times10^{-3}$	5.652×10^{-3}	9.0
2743 (9,000 ft)	3048 (10,000 ft)	$\sigma_9 = 2.14\times10^{-3}$	3.531×10^{-3}	4.5
3048 (10,000 ft)	3353 (11,000 ft)	$\sigma_{10} = 2.23\times10^{-3}$	2.2319×10^{-3}	3.0
3353 (11,000 ft)	3656 (12,000 ft)	$\sigma_{11} = 2.17\times10^{-3}$	1.422×10^{-3}	1.8
3656 (12,000 ft)	3962 (13,000 ft)	$\sigma_{12} = 2.25\times10^{-3}$	9.141×10^{-4}	1.2
3962 (13,000 ft)	4267 (14,000 ft)	$\sigma_{13} = 2.25\times10^{-3}$	5.911×10^{-4}	0.8
4267 (14,000 ft)	4572 (15,000 ft)	$\sigma_{14} = 1.84\times10^{-3}$	3.844×10^{-4}	0.4
4572 (15,000 ft)	4877 (16,000 ft)	$\sigma_{15} = 1.56\times10^{-3}$	2.512×10^{-4}	0.2

* $$I_i = \int_{r_{i-1}}^{r_i} \frac{e^{-r/850}}{r}\, dr \quad .$$

In practice, this value will give an upper limit to the population dose equivalent because:

a. The population density estimates used in the calculation are conservative.

b. The value of population dose equivalent depends strongly upon the value of λ assumed. In the calculations presented here, a value of λ = 850 meters has been used. This value is appropriate for that component of the fence post dose equivalent contributed by the Bevatron and 184-inch cyclotron. The contribution of the SuperHILAC and 88-inch cyclotrons to the population dose will overestimate in the ratio $\approx (850/250)^{2/3}$, or a little more than a factor of two. If these two accelerators contribute a proportion, f, of the minimum fence post dose equivalent, the population dose equivalent is then more accurately written:

$$M = 1000\ H_0 \left[(1 - f) + \left(\frac{250}{850}\right)^{2/3} f \right]$$

$$= 1000\ H_0\ [1 - 0.56\ f] \qquad (15)$$

c. In calculating M the maximum value of H_0 is used. There are uncertainties in this value of H_0 comparable with the value of annual fence post dose equivalent itself. Choice of the maximum value of H_0 may, therefore, greatly overestimate the true value of population dose equivalent.

For these reasons we feel justified in expressing the population dose equivalent due to high-energy accelerator operation at LBL as:

$$M/H_0 \leq 1000 \text{ man-rem/fence post rem}$$

4.3. Model for Estimating the Population Dose Equivalent Resulting from the Release of Radionuclides

4.3.1. General

The calculation of population exposure resulting from the release of radionuclides from a nuclear facility requires:

a. An estimate of the total quantity of radionuclides released or the rate of release.

b. Calculations of the atmospheric concentrations of radionuclides in the atmosphere, resulting from these releases, as a function of position at locations where people may be exposed.

c. Conversion of the atmospheric concentrations to dose equivalent to an exposed individual.

d. Summation of the total number of exposed individuals and their dose equivalent to give the total population dose.

The quantities of radionuclides released to the atmosphere from the Laboratory are, in general, very small and occur quite randomly in time. In such a case it is sufficiently accurate to assume an average continuous rate of emission under average meteorological conditions. This section describes the model used to estimate population dose equivalent resulting from radionuclides released from LBL.[85]

4.3.2. Concentration of Radionuclides in the Atmosphere

It is convenient to divide the region surrounding the Laboratory into sectors as shown in Fig. 16. The time integrated concentration, ψ (often referred to as the exposure), of a radionuclide at distance r from the source is then well known to be:[86]

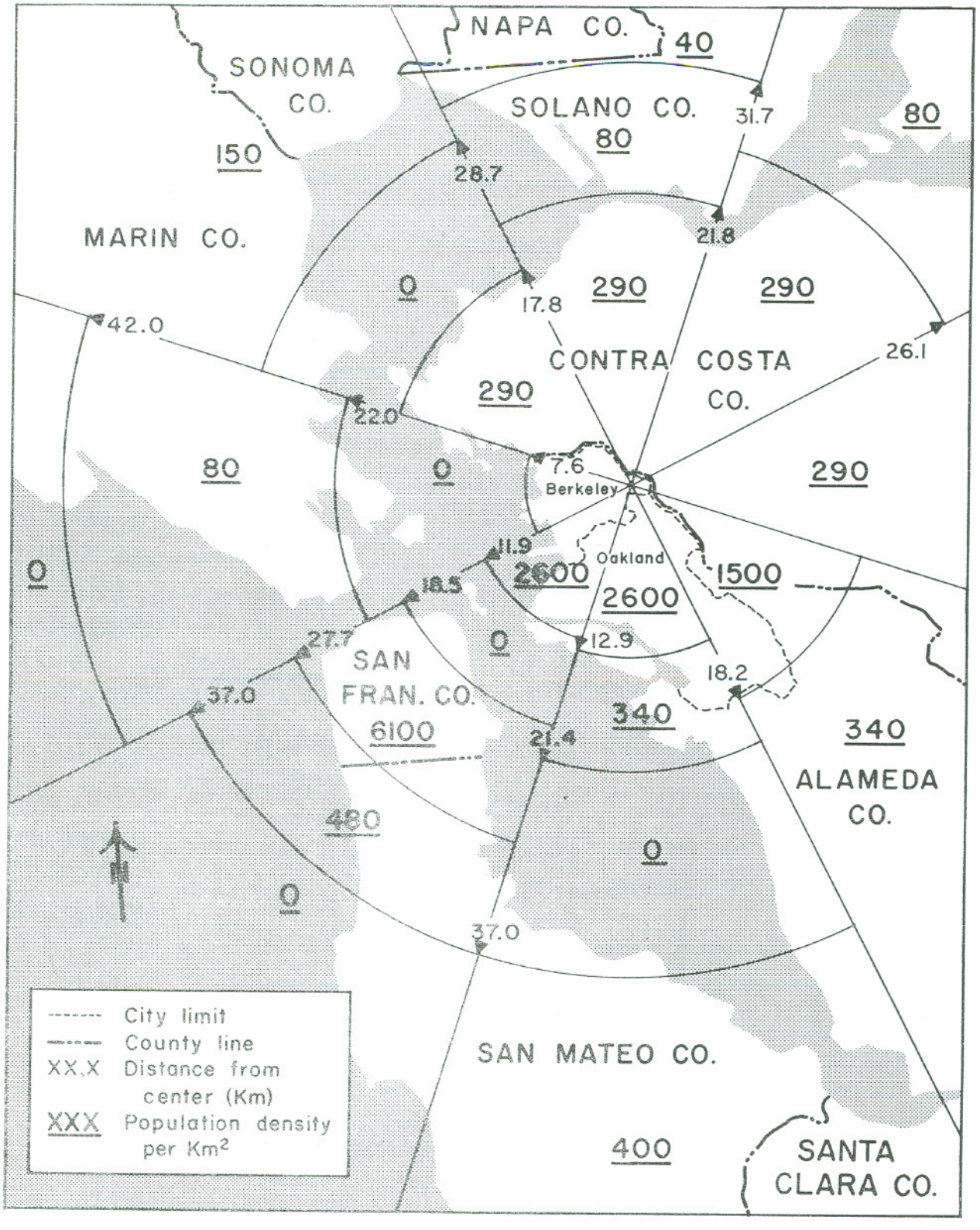

XBL 764-1360

Fig. 16. Population zones in San Francisco Bay Region used in calculation of population dose equivalent due to release of radionuclides.

$$\Psi(r) = \sqrt{\frac{2}{\pi}} \left(\frac{n}{2\pi r}\right) \cdot \frac{fQ}{\sigma_z(r)\bar{u}} \exp\left(-\frac{h^2}{2\sigma_z(r)^2}\right) \tag{16}$$

where n = number of sectors

f = fraction of total time in which the wind blows towards a given sector

$\frac{2\pi r}{n}$ = sector width

$\bar{u}$ = average wind velocity (meters sec^{-1})

h = height of stack above ground level (meters)

$\sigma_z(r)$ = vertical dispersion coefficient (meters)

Q = total quantity of radionuclides released (curies)

In the case where h is zero (which is true at LBL), Eq. (16) becomes:

$$\Psi(r) = \sqrt{\frac{2}{\pi}} \left(\frac{n}{2\pi r}\right) \cdot \frac{fQ}{\sigma_z(r)\bar{u}} \tag{17}$$

With Q in curies, r and σ_2 in meters, $\bar{u}$ in meters/sec, Ψ will have the units of curie sec/cubic meter.

4.3.3. Dose Equivalent to an Individual

Exposure to a given radionuclide may be related to dose equivalent, H, by a simple proportionality factor R:

$$H(r) = R\Psi(r) \tag{18}$$

Values of R for various radionuclides are available in the literature.[87]

With M in units of man rem and $\Psi(r)$ in curie seconds per cubic meter, R has the units rem cubic meters per curie second.

4.3.4. Population Dose Equivalent

The population dose equivalent in the i^{th} sector, M_i, is given by:

$$M_i = \int_{r_0}^{\infty} R\, \Psi_i(r)\, N_i(r)\, dr \qquad (19)$$

where $\Psi_i(r)$ is the total exposure to the radionuclide in the i^{th} sector, at distance r from the source and is given by Eq. (17) and $N_i(r)\, dr$ is the total number of people in the i^{th} sector in the region between r and r + dr. r_0 is the distance of closest approach to the Laboratory.

Substituting for $\Psi(r)$ from Eq. (17) we obtain:

$$M_i = \sqrt{\frac{2}{\pi}} \left(\frac{n}{2\pi}\right) \frac{f_i Q R}{\bar{u}} \int_{r_0}^{\infty} \frac{N_i(r)}{r\sigma_z(r)}\, dr \qquad (20)$$

The total population dose equivalent M is than given by:

$$M = \sum_{i=1}^{n} M_i \qquad (21)$$

Evaluation of the population dose equivalent thus requires:

1. Evaluation of the meterological parameters $\bar{u}$ and f_i.
2. Determination of the variation of the vertical dispersion coefficient, $\sigma_z(r)$, with distance.
3. Evaluation of population as a function of distance and direction from the Laboratory

4.3.5. Average Meteorological Conditions

Average wind speed and the frequency of direction derived from 2805 observations, made at 3 hourly intervals for eight sectors, taken during 1975 are summarized in Table 13.[85] The overall average wind speed during 1975 was 1.7 meters sec^{-1}.

Table 13. Frequency of Observation of Wind Blowing from Given Direction during 1975.

Direction	Relative Frequency
N	0.093
NE	0.042
E	0.039
SE	0.105
S	0.183
SW	0.091
W	0.204
NW	0.191
Calms	0.052
	1.000*

*Overall average wind speed 1.7 meters per second.

4.3.6. Variation of Vertical Dispersion Coefficient with Distance

Figure 17 shows values of σ_z as a function of distance from the source for the most typical atmospheric stability condition observed at LBL during 1975, which was Pasquill's category F (moderately stable). The curve for this atmospheric condition (Fig. 17) may be approximated by the expressions:

$$\sigma_z(r) = 0.055\ r^{0.81} \quad 100 \text{ meters} \leq r \leq 2{,}000 \text{ meters} \qquad (22)$$

$$= 1.75\ r^{0.353} \quad 2{,}000 \text{ meters} \leq r \leq 10{,}000 \text{ meters} \qquad (23)$$

4.3.7. Population Distribution Around the Lawrence Berkeley Laboratory

The availability of meteorological information of eight sectors make these regions natural subdividisions for the determination of population.

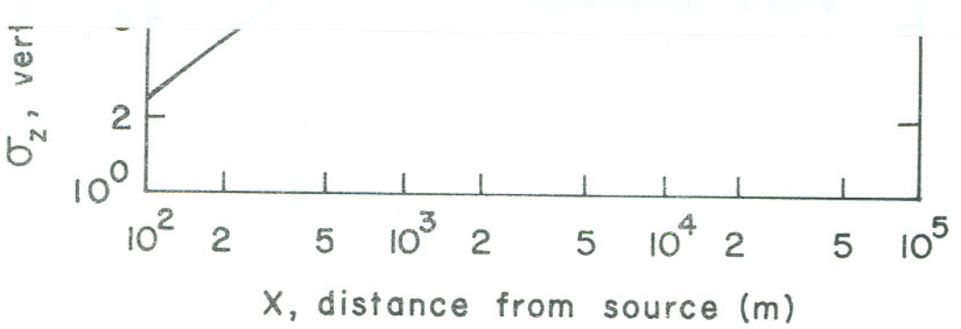

XBL 764-1359

Fig. 17. The vertical dispersion coefficient, σ_z, as a function of distance from the source for Pasquill's turbulence type F.

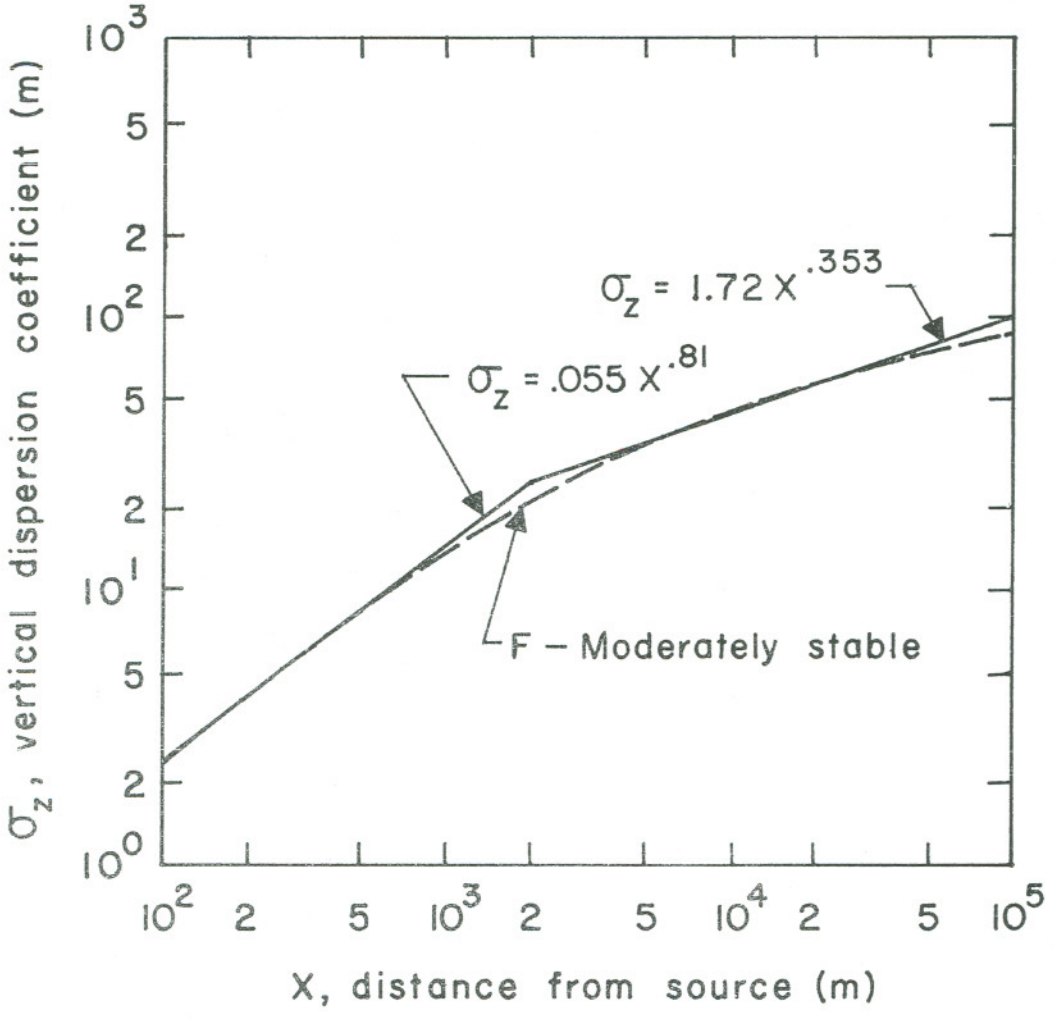

XBL 764-1359

Fig. 17. The vertical dispersion coefficient, σ_z, as a function of distance from the source for Pasquill's turbulence type F.

Table 14 summarizes the population, area, and population densities for the counties of the San Francisco Bay region.[88] From these data the eight sectors were subdivided into regions in which the population density could reasonably be assumed to be constant. The average population densities derived for these regions are summarized in Table 15.

Table 14. Population and Area Data for the San Francisco Bay Region.

Political Unit	Population	Land Area (Square Miles)	Population Density (m^{-1})
City of Berkeley	116,716	10.16	$4.4\ 10^{-3}$
City of Oakland	361,561	53.44	$2.6\ 10^{-3}$
Alameda County, excluding Oakland and Berkeley	594,907	670.0	$3.4\ 10^{-4}$
Contra Costa County	555,805	735.0	$2.9\ 10^{-4}$
Marin County	206,758	520.0	$1.5\ 10^{-4}$
Napa County	79,140	787.0	$3.9\ 10^{-5}$
San Francisco County	715,674	45.0	$6.1\ 10^{-3}$
San Mateo County	556,805	447.0	$4.8\ 10^{-4}$
Santa Clara County	1,068,174	1300.0	$3.2\ 10^{-4}$
Solano County	171.989	823.0	$8.1\ 10^{-5}$
Sonoma County	204,885	1604.0	$4.9\ 10^{-5}$

(From 1970 census figures, as shown in World Almanac.) Total population within 50 miles of LBL is about 4.5 million.

An internal check of the data in Table 15 calculated the total population of the Bay Area as 4.9 million--in reasonable agreement with the actual population of 4.5 million.

4.3.8. Population Dose Equivalent Around the Lawrence Berkeley Laboratory

Evaluation of the M_i's defined by Eq. (20) is possible by the subdivision of each sector into regions in which the population density may be assumed constant.

The number of residents at distance r from the Laboratory in the j^{th} region of the i^{th} sector, ${}_jN_i(r)\,dr$ is then given by:

$$ {}_jN_i(r) = \frac{2\pi r}{n}\,\sigma_{ij}\,dr \qquad (24) $$

where σ_{ij} is the population density.

Substituting Eq. (24) into Eq. (20) we obtain the population dose equivalent in the j^{th} region of the i^{th} sector ${}_jM_i$ is given by:

$$ {}_jM_i = \sqrt{\frac{2}{\pi}}\;\frac{f_i Q R \sigma_{ij}}{\bar{u}} \int_{r_{j-1}}^{r_j} \frac{dr}{\sigma_z(r)} \qquad (25) $$

Substituting the expressions for $\sigma_z(r)$ (Eqs. (22) and (23) we obtain:

$$ {}_jM_i = 76.4\left(\frac{f_i\sigma_{ij}}{\bar{u}}\right) RQ \left\{ r_j^{0.19} - r_{j-1}^{0.19} \right\} \quad r \leq 2{,}000 \text{ meters} $$

$$ = 0.715\left(\frac{f_i\sigma_{ij}}{\bar{u}}\right) RQ \left\{ r_j^{0.647} - r_{j-1}^{0.647} \right\} \quad r \geq 2{,}000 \text{ meters} $$

(r in meters) (26)

$$M = \sum_{i=1}^{n} M_j$$

$$= \sum_{i=1}^{n} \sum_{j=1}^{m} {}_jM_i \qquad (27)$$

Table 15 summarizes the numerical values obtained in the evaluation of population dose equivalent.

It is convenient to define a parameter α defined by the equation:

$$\alpha = \frac{M_k}{QR_k}$$

where M_k is the population dose equivalent resulting from the release of Q curies of a radionuclide, k. For the Lawrence Berkeley Laboratory α has the numerical value:

$$\alpha = \underline{0.421}$$

Table 16 summarizes values of the factors, R, used to convert exposure to dose equivalent.

Table 15. Data for the Calculation of Population Dose Equivalent Due to the Release of Radionuclides.

Sector	Wind Frequency, f	Region (Radii in Kilometers)		Pop Density, km^{-2}	
		r_1	r_2	σ_{ij}	α
NE	0.042	0.0	26.1	290	0.0115
NE	0.042	26.1	80.0	80	0.0023
E	0.039	0.0	80.0	290	0.0448
SE	0.105	0.0	18.2	1500	0.1066
SE	0.105	18.2	80.0	340	0.0250
S	0.183	0.0	12.9	2600	0.0784
S	0.183	12.9	21.4	340	0.0024
S	0.183	21.4	37.0	0	0.0000
S	0.183	37.0	80.0	400	0.0091
SW	0.091	0.0	11.9	2600	0.0343
SW	0.091	11.9	18.5	0	0.0000
SW	0.091	18.5	27.7	6100	0.0185
SW	0.091	27.7	37.0	480	0.0013
SW	0.091	37.0	80.0	0	0.0000
W	0.204	0.0	7.6	4400	0.0460
W	0.204	7.6	22.0	0	0.0000
W	0.204	22.0	42.0	80	0.0004
W	0.204	42.0	80.0	0	0.0000
NW	0.191	0.0	17.8	290	0.0112
NW	0.191	17.8	28.7	0	0.0000

Table 15. Continued.

Sector	Wind Frequency, f	Region (Radii in Kilometers) r_1	r_2	Pop Density, km^{-2} σ_{ij}	α
NW	0.091	28.7	80.0	150	0.0048
N	0.093	0.0	21.8	290	0.0213
N	0.093	21.8	31.7	80	0.0011
N	0.093	31.7	80.0	40	0.0021
					0.4212

Table 16. Population Dose Equivalent Resulting from the Release of 1 Curie of Radionuclides.

Radionuclide	R (Ref. 84) rem m^3 Ci^{-1} s^{-1}	αR man rem/Ci
^{3}H*	0.0286	0.0120
Unidentified alpha** Emitters	36,100	15,200
Unidentified β*** Emitters	532	224
^{14}C	0.0966	0.0407

*In the form of HTO.

**^{239}Pu used as a conservative value.

***^{90}Sr used as a conservative value.

REFERENCES

1. Smith, A. R. and Wollenberg, H. A., Lawrence Berkeley Laboratory, Private Communication (January 1974).

2. Ionizing Radiation, Levels and Effects. Vol. 1, Levels, UNSCEAR Report, United Nations, New York (1972). See also: Natural Background Radiation in the United States, NCRP Report No. 45, National Council on Radiation Protection and Measurements, Washington, D.C., November 1975.

3. Stephens, L. D. and Cantelow, H., Annual Environmental Monitoring Report, Lawrence Berkeley Laboratory Report LBL-3821, April 1975.

4. Wollenberg, H. A. and Smith, A. R., Geologic Factors Controlling Terrestrial Gamma-Ray Dose Rates, Lawrence Berkeley Laboratory Report LBL-914, July 1972.

5. Beck, H. L., Lowder, W. M., Bennet, B. G., and Condon, W. J., Further Studies of Environmental Radiation, Health and Safety Laboratory Report, HASL-170 (1966).

6. Wollenberg, H. A. and Smith, A. R., Studies in Terrestrial Gamma Radiation; Chapter 32 in J. A. S. Adams and W. Lowder (eds), The Natural Radiation Environment, University of Chicago Press, 1964).

7. Smith, A. R. and Wollenberg, H. A. Detailed Radiogeologic Survey of the Natural Gamma-Radiation Environment at the Lawrence Berkeley Laboratory Site, Lawrence Berkeley Laboratory Report LBL-3642.

8. de Planque Burke, G., Variations in Natural Environmental Gamma Radiation and its Effect on the Interpretability of TLD Measurements Made Near Nuclear Facilities, Health and Safety Laboratory Report, HASL-289 (1975).

9. de Planque Burke, G., A Model for Estimating Variations in Terrestrial Radiation Exposures Based on Soil-Water Balance, Chapter XII in Second Workshop on the Natural Radiation Environment, Wayne M. Lowder, editor, Health and Safety Laboratory Report HASL-287, September 1974.

10. Smith, A. R., Lawrence Berkeley Laboratory, Private Communication, December 1975.

11. G. E. Jones and L. M. Kleppe, A Simple and Inexpensive System for Measuring Concentrations of Atmospheric Radon-222; Lawrence Radiation Laboratory Report UCRL-16952 (1966).

12. Hess, W. N., Canfield, E. H., and Lingenfelter, R. E., Cosmic-Ray Neutron Demography, Journal of Geophysical Res., vol. 6, no. 3, March 1961, pp. 665-677.

13. Kent, R. A. R., Cosmic Ray Neutron Measurements, USAEC Rept., HW-SA-2870, May 25, 1963.

14. Boella, G., Antoni, G. Degli, Dilworth, C., Giannelli, G., Rocca, E., Scarsi, L., and Shapiro, D., Measurement of the Cosmic-Ray Neutron Flux in the Atmosphere, II Nuovo Cimento, vol. 29, no. 1, July 1, 1963, pp. 103-117.

15. Yamashita, Mikio., Stephens, Lloyd D., and Patterson, H. Wade, Cosmic-Ray-Produced Neutrons at Ground Level: Neutron Production Rate and Flux Distribution, J. Geophys. Res., vol. 71, no. 16, Aug. 15, 1966, pp. 3817-3834.

16. Hajnal, Ferenc., McLaughlin, James E., Weinstein, Martin S., O'Brien, Keran, 1970 Sea-Level Cosmic-Ray Neutron Measurements, USAEC Rept. HASL-241, Feb. 1971.

17. Anon: Report of the United Nations Scientific Committee on the Effects of Atomic Radiation. General Assembly, Official Records: 21st Session, Supplement 14 (A/6314). United Nations Scientific Committee on the Effects of Atomic Radiation, New York, 1966.

18. Boella, G., Antoni, G. Degli, Dilworth, C., Panetti, M., and Scarsi, L., Measurement of the Cosmic Ray Neutron Flux at 4.6 Billion Volts Geomagnetic Cutoff Rigidity, J. Geophys. Res., vol. 70, no. 5, March 1, 1965, pp. 1019-1030.

19. Watt, D. E., Clare, D. M., Gordon, A. R. B., Tissue Dose-Equivalent Rates. I. From Cosmic Ray Neutrons. II. In the Low Level Environment of Chapelcross Nuclear Power Station. UKAEA Rept. PG-Report-734, 1965.

20. Hewitt, J. E., et al., Ames Collaborative Study of Cosmic Ray Neutrons, NASA Technical Memorandum, NASA TM X-3329, January 1976.

21. Shaw, K. B., Stevenson, G. R., and Thomas, R. H., Evaluation of Dose Equivalent from Neutron Energy Spectra, Health Physics 17, 459 (1969).

22. Stephens, L. D., Patterson, H. W., and Smith, A. R., Fallout and Natural Background in the San Francisco Bay Area, Health Physics 4, 267 (1961).

23. Wollenberg, H. A., Patterson, H. W., Smith, A. R., and Stephens, L. D., Natural and Fallout Radioactivity in the San Francisco Bay Area, Health Physics 17, 313 (1969).

24. Local Climatological Data--Annual Summary with Comparative Data, Oakland, CA (National Oceanic and Atmospheric Administration, Environmental Data Service, National Climatic Center, Asheville, NC) 1974.

25. Cantelow, H. P., Lawrence Berkeley Laboratory, Private Communication. March 1976.

26. Peak, J. S., Cantelow, H. P., Young, J., and Latimer, R. M., Wind Data Summary, Lawrence Radiation Laboratory, Berkeley, UCRL-20224 (December 1970).

27. Air Pollution and the San Francisco Bay Area, Bay Area Air Pollution Control District, 6th Edition, March 1972.

28. Cantelow, Herbert P., Peak, J. S., Salo, A. E., and Howe, P. W., Environmental Sampling at Lawrence Radiation Laboratory, Berkeley, UCRL-10255, 1962.

29. Zaitsev, L. N., Komochkov, M. M. and Sychev, B. C., The Basis of Accelerator Shielding (in Russian), Atomizdat, Moscow (1971).

30. Freytag, E., Radiation Protection at High Energy Accelerators (in German), G. Braun, Karlsruhe (1972).

31. Patterson, H. W., and Thomas, R. H., Accelerator Health Physics, Academic Press, NY (1973).

32. Patterson, H. W., and Thomas, R. H., Experimental Shielding Studies at High Energy Accelerators--A Review, Particle Accelerators 2, 77 (1971).

33. Thomas, R. H., Neutron Dosimetry at High Energy Particle Accelerators--A Review, Lawrence Berkeley Laboratory internal Report LBL-986 (October 1972). Proceedings of IAEA Symposium on Neutron Monitoring, Vienna, December 11-15, 1972, vol. 1, p. 352, IAEA Vienna (1973).

34. Rindi, A., and Thomas, R. H., The Radiation Environment of High Energy Accelerators, Ann. Rev. Nucl. Sci. 23, 315 (1973).

35. McCaslin, J. B., Bevatron Survey--March 1966, Private Communication.

36. Patterson, H. W., The Effect of Shielding Produced by the 730 MeV Synchrocyclotron and the 6.3 GeV Proton Synchrotron at the Lawrence Radiation Laboratory, in Proceedings of the Premier Colloque International sur la Protection Aupres des Grands Accelerateurs Presses Universitaires de France, Paris 1962, p. 95.

37. Rindi, A. and Thomas, R. H., Skyshine, Particle Accelerators 7, 23 (1975).

38. Nelson, W. R., Radioactive Ground Water Produced in the Vicinity of Beam Dumps, Stanford Linear Accelerator Center Internal Report SLAC TN, July 1965 (unpublished).

39. Busick, D., A Ten-Year Summary of Environmental Radiation Measurement at SLAC, to be published.

40. Hoyer, F., Induced Radioactivity in the Earth Shielding on Top of High Energy Particle Accelerators, CERN 68-42, December 9, 1968.

41. Thomas, R. H., Possible Contamination of Ground Water System by High Energy Proton Accelerators, in Proceedings of the Symposium on Health Physics Aspects of Nuclear Facility Siting, Idaho Falls, November 3-6, 1970.

42. Borak, T. B., et al., The Underground Migration of Radionuclides Produced in Soil Near High Energy Proton Accelerators, Health Physics 23, 679 (1972).

43. Stapleton, G. B., and Thomas, R. H., Estimation of the Induced Radioactivity of the Ground Water System in the Neighborhood of a Proposed 300-GeV High Energy Accelerator Situation on a Chalk Site, Health Physics 23, 689 (1972).

44. Stapleton, G., and Thomas, R. H., The Production of ^{7}Be by 7-GeV Proton Interactions with Oyxgen, Nucl. Phys. A175, 124 (1971).

45. Stapleton, G., and Thomas, R. H., The Effect of Sorption on the Migration of ^{7}Be from a High Energy Accelerator Constructed on a Chalk Site, Water Research 7, 1259 (1973).

46. Thomas, R. H., Radioactivity in Earth Induced by High Energy Electrons, Nucl. Inst. Methods 102, 149 (1972).

47. Mawson, C. A., Consequences of Radioactive Disposal into the Ground in Health Physics, vol. 2. pt. 1, A. M. F. Duhamel (ed), Pergamon Press, Oxford (1969).

48. Patterson, H. W., and Thomas, R. H., Accelerator Health Physics, Chapter 7, p. 539, Academic Press, New York (1973).

49. Brookhaven National Laboratory, Advanced Accelerator Department, Proposal for Increasing the Intensity of the AGS at the Brookhaven National Laboratory, Internal Report BNL-7956 (May 1964).

50. George, A. G., Breslin, A. J., Hoskins, J. W., and Ryan, R. M., Proc. First Symposium on Accelerator Radiation Dosimetry, Brookhaven National Laboratory, CONF-65119, 1969, pp. 513-555.

51. Rindi, A., and Charalambus, S., Airborne Radioactivity Produced at High Energy Accelerators, Nucl., Inst. and Methods 47, 227 (1967).

52. Charalambus, S., and Rindi, A., Aerosol and Dust Radioactivity in the Halls of High Energy Accelerators, Nucl. Inst. and Methods 56, 125 (1967).

53. Shaw, K. B., and Thomas, R. H., Problems Associated with High Energy Proton Beams, Health Physics 13, 1127 (1967).

54. Ladu, M., Pellicioni, M., and Roccella, M., Produzione e Scarcio di Gas Tossici e Radioattiviti nel Tunnel del Linac di Frascati, Giornale di Fisica Sanitari-Minerva Fisico-Nucleare 11, No. 2, 112 (1967).

55. Awschalom, M., Larsen, F. L., and Schimmerling, W., Activation of Air Near a Target Bombarded by 3-GeV Protons, Princeton Report PPAD-661E, May 1969.

56. Höfert, M., Radiation Hazard of Induced Activity in Air as Produced by High Energy Accelerators, in Proc. Second Int. Conf. on Accelerator Dosimetry, Stanford, November 1969, CONF-691101, p. 111.

57. Viallettes, H., Gas and Dust Activation in the Target Room of the Saclay Electron Linac, in Proc. Second Int. Conf. on Accelerator Dosimetry, Sanford, November 1969, CONF-691101, p. 121.

58. Warren, G. J., Busick, D. D., and McCall, R. C., Radioactivity Produced and Released from Water at High Energies, in Proc. Second Int. Conf. on Accelerator Dosimetry, Stanford, November 1969, CONF-601101, p. 99.

59. Rindi, A., La Radioactivité Induite Dans l'Air de l'Accelerateur de Protons de 300-GeV du CERN, CERN Internal Note, CERN Lab II, RA-72/5 (1972).

60. Peetermans, A., and Baarli, J., Radioactive Gas and Aerosol Production by the CERN High Energy Accelerators and the Evaluation of its Influence on the Environmental Problems, CERN Internal Note, DI/HP/174, October 1973.

61. Smith, A. R., Lawrence Berkeley Laboratory, Private Communication, 1974.

62. Patterson, H. W., Private Communication (1974).

63. Recommendations for the International Commission on Radiological Protection, ICRP Publication No. 9 (Pergamon, London, 1966), p. 14.

64. Stephens, L. D., and Dakin, H. S., A High Reliability Environmental Radiation Monitoring System, Proc. of the VIth Intern. Congress of the Societe Francaise de Radioprotection, Bordeaux, France (March 27-31, 1972), p. 753.

65. Jones, A. R., Pulse Counter for Gamma Dosimeters, Health Physics 8, 9 (1962).

66. Wallace, R. W., Moyer, B. J., Patterson, H. W., Smith, A. R., and Stephens, L. D., The Dosimetry of High-Energy Neutrons Produced by 6.2 GeV Protons Accelerated in the Bevatron, in Proc. of Selected Topics in Radiation Dosimetry, IAEA, Vienna, 1961, p. 579.

67. McCaslin, J. B., Patterson, H. W., Smith, A. R., and Stephens, L. D., Some Recent Developments in Technique for Monitoring High-Energy Accelerator Radiation, in Proc. of the First IRPA Symp., Rome, September 5-10, 1966, Pergamon Press, New York (1968), p. 1131

68. Thomas, R. H., Implementing the Requirement to Reduce Radiation Exposure to "As Low As Practicable" at the Lawrence Berkeley Laboratory, Health Physics 30 271 (1976).

69. International Commission on Radiation Units and Measurements, Radiation Protection Instrumentation and Application, ICRU Report 20, Section I.C.6., Washington, D.C.

70. Beck, H. L., DeCampo, J., and Gogolak, C., "In-Situ Ge (Li) and NaI (Tl) Gamma-Ray Spectrometry," USAEC Health and Safety Laboratory Report HASL-258 (1972).

71. Phelps, P. L., Anspaugh, L. R., Roth, S. J., Huckabay, G. W., and Sawyer, D. L., Ge (Li) Low Level In-Situ Gamma-Ray Spectrometry Applications, in IEEE Trans. on Nucl. Sci., NS-21, No. 1, p. 543, February 1974.

72. Data for protection against ionizing radiation from external sources, ICRP Publication 21, Pergamon, London (1973).

73. Gilbert, W. S., et al., 1966 CERN-LRL-RHEL Shielding Experiment, Lawrence Radiation Laboratory Internal Report UCRL-17941 (1968).

74. Natural Background Radiation in the United States, NCRP Report No. 45, National Council on Radiation Protection and Measurements, Washington, D.C., November 1975, Chapter 3.

75. Radin, J. R., Gradsztajn, E., and Smith, A. R., ^{7}Be Production Cross Sections in ^{14}N, ^{12}C, ^{11}B, and ^{10}B with 740-MeV Protons, Lawrence Berkeley Laboratory Internal Report, LBL-2680, March 1974.

76. ICRP Implications of Commission Recommendations that Doses be Kept as Low As Readily Achievable, ICRP Publication 22, Pergamon Press, Oxford (1973).

77. Stephens, L. D., Thomas, R. H., and Thomas, S. B., Population Exposure from High Energy Accelerators, Health Physics 29, 853 (1975).

78. Thomas. S. B., Distribution of Population Around Lawrence Berkeley Laboratory, Health Physics Department, Lawrence Berkeley Laboratory Internal Note HPN/23 (January 10, 1975).

79. 1970 Census of Housing--Block Statistics of San Francisco-Oakland, CA Urbanized Area, U. S. Department of Commerce, Bureau of Census Report HC(3)-24 (December 1971).

80. Campus Statistics, Fall Quarter 1973 and Year 1972-1973, University of California, Berkeley, Office of Institutional Research (April 1974).

81. Stephens, L. D. and Thomas, R. H., Estimate of Population Exposure due to Operation of the Lawrence Berkeley Laboratory Particle Accelerator, Health Physics Department, Lawrence Berkeley Laboratory Internal Report UCID-3602 (April 24, 1973).

82. Personnel Listing, University of California, Berkeley, Office of Analytical Studies, P. A. Series 604 (April 1973).

83. J. B. McCaslin, Health Physics Department, Lawrence Berkeley Laboratory, Private Communication.

84. Stephens, L. D., Thomas, S. B., and Thomas, R. H., A Model for Estimating Population Exposures due to the Operation of High-Energy Accelerators at the Lawrence Berkeley Laboratory, March 1975, submitted to Health Physics.

85. Cantelow, H., Calculation of Man-Rem from Radioisotope Release from LBL to the Atmosphere, Safety Services Department LBL Internal Document (February 26, 1976), HPC:047:76.

86. See for example, Meteorology and Atomic Energy (D. H. Slade (ed)), USAEC, Division of Techinfo., July 1968, TID-24190.

87. D. F. Bunch, Dose to Various Body Organs from Inhalation or Ingestion of Soluble Radionuclides, IDO-12054, August 1966.

88. World Almanac. Newspapers Enterprise Association, Inc., New York and Cleveland (1975).

DISTRIBUTION

Internal		Copies
A. M. Sessler	Director's Office	2
E. K. Hyde		2
W. D. Hartsough		2
G. L. Pappas		2
E. L. Alpen - Associate Director, Biology and Medicine Division		1
R. W. Birge - Associate Director, Physics, Computer Science and Mathematics Division		1
R. J. Budnitz - Acting Head, Energy and Environment Division		1
B. G. Harvey - Associate Director, Nuclear Science Division		1
Health Physics Department		50
Safety Services Department		3
Lawrence Hall of Science		3
Technical Information Department		15
External		
UC-11 Environmental Control Technology and Earth Sciences		182
Federal Agencies		
ERDA Headquarters		1
ERDA San Francisco Operations Office		1
Regional Administrator, EPA--Region IX		1
State of California and Local Public Health Agencies		
Bureau of Radiological Health		2
Public Health Agencies:		
Berkeley		1
Oakland		1
San Francisco		1
Alameda County		1
Bay Area Air Pollution Control District		1
A. Hull - Brookhaven National Laboratory		1
D. Busick - Stanford Linear Accelerator Center		1
P. Gollon - Fermi National Accelerator Laboratory		1
D. Jacobs - Oak Ridge National Laboratory		1
J. Sedlet - Argonne National Laboratory		1